Cell Reports
Methods

Article

# Diagnostic TR-FRET assays for detection of antibodies in patient samples

## Graphical abstract

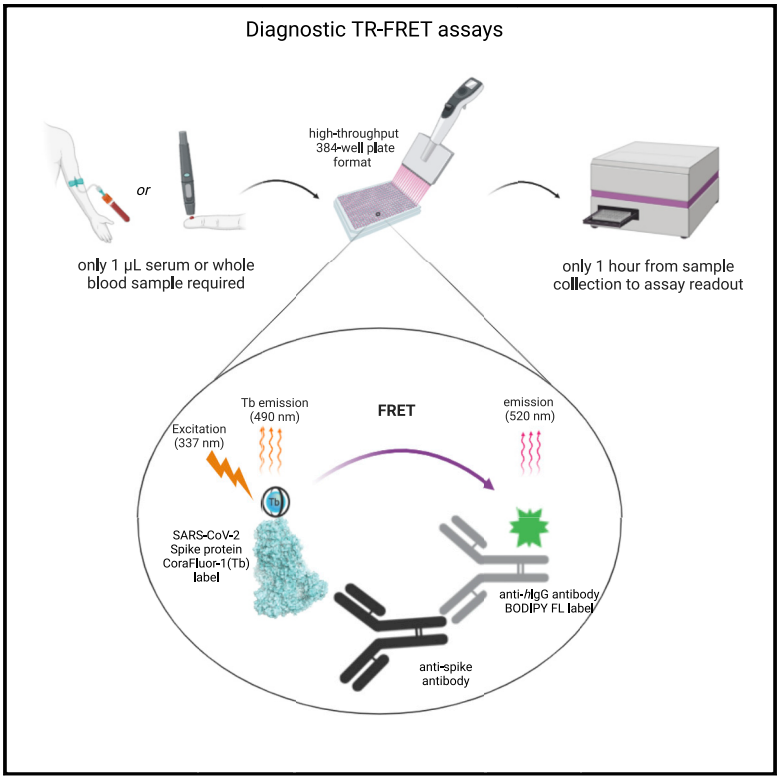


## Highlights

- Homogeneous TR-FRET assay can accurately detect IgG levels in patient serum samples
- TR-FRET assay can rapidly be extended to survey antibodies against different antigens
- TR-FRET assay is compatible with diverse serological sample types

## Authors

Hong Yue, Radosław P. Nowak, Daan Overwijn, ..., Galit Alter, Ralph Mazitschek, Eric S. Fischer

## Correspondence

eric_fischer@dfci.harvard.edu

## In brief

Yue et al. develop a homogeneous TR-FRET assay for the detection of antibodies for specific antigens in human serum, plasma, and blood samples. The assay requires only a 1 µL sample, spans 1 h from sample to readout, and is easily adaptable to new antigens.

Yue et al., 2023, Cell Reports Methods 3, 100421
March 27, 2023 
https://doi.org/10.1016/j.crmeth.2023.100421

CellPress

Cell Reports Methods

CellPress
OPEN ACCESS

Article

# Diagnostic TR-FRET assays for detection of antibodies in patient samples

Hong Yue,[1,2,11] Radosław P. Nowak,[1,2,11] Daan Overwijn,[1,2] N. Connor Payne,[3,4] Stephanie Fischinger,[5] Caroline Atyeo,[5] Evan C. Lam,[5] Kerri St. Denis,[5] Lauren K. Brais,[6] Yoshinobu Konishi,[6,7] Romanos Sklavenitis-Pistofidis,[6,7] Lindsey R. Baden,[8] Eric J. Nilles,[9] Elizabeth W. Karlson,[10] Xu G. Yu,[5] Jonathan Z. Li,[8] Ann E. Woolley,[8] Irene M. Ghobrial,[6,7] Jeffrey A. Meyerhardt,[6] Alejandro B. Balazs,[5] Galit Alter,[5] Ralph Mazitschek,[4,7] and Eric S. Fischer[1,2,12,*]

[1]Department of Cancer Biology, Dana-Farber Cancer Institute, Boston, MA 02215, USA
[2]Department of Biological Chemistry and Molecular Pharmacology, Harvard Medical School, Boston, MA 02115, USA
[3]Department of Chemistry & Chemical Biology, Harvard University, Cambridge, MA 02138, USA
[4]Center for Systems Biology, Massachusetts General Hospital (MGH), Boston, MA 02114, USA
[5]Ragon Institute of MGH, Massachusetts Institute of Technology (MIT), and Harvard, Cambridge, MA 02139, USA
[6]Department of Medical Oncology, Dana-Farber Cancer Institute, Boston, MA 02215, USA
[7]Broad Institute of MIT and Harvard, Cambridge, MA 02142, USA
[8]Division of Infectious Diseases, Brigham and Women's Hospital, Boston, MA 02115, USA
[9]Department of Emergency Medicine, Brigham and Women's Hospital, Boston, MA 02115, USA
[10]Department of Medicine, Brigham and Women's Hospital, Boston, MA 02115, USA
[11]These authors contributed equally
[12]Lead contact
*Correspondence: eric_fischer@dfci.harvard.edu
https://doi.org/10.1016/j.crmeth.2023.100421

**MOTIVATION** Monitoring immune response is a crucial component of management and tracking of the spread of infectious diseases. Current serological testing laboratory assays are limited by the need for specialized automation, sample types, and cost. Time-resolved Förster energy transfer (TR-FRET) homogeneous assays provide an alternative, but their scope and limitations have not been extensively tested in a large-scale study. To address this, we have developed a suite of TR-FRET-based serological assays used to detect antigen-specific antibodies as well as total IgG levels, validated them in a large cohort study (>1,500 samples), and showed that they maintain high reproducibility and repeatability. TR-FRET assays perform on par or better than alternative laboratory tests that have previously been evaluated on the same set of samples while reducing the time to result (<1 h) and the costs per sample.

## SUMMARY

Serological assays are important diagnostic tools for surveying exposure to the pathogen, monitoring immune response post vaccination, and managing spread of the infectious agent among the population. Current serological laboratory assays are often limited because they require the use of specialized laboratory technology and/or work with a limited number of sample types. Here, we evaluate an alternative by developing time-resolved Förster resonance energy transfer (TR-FRET) homogeneous assays that exhibited exceptional versatility, scalability, and sensitivity and outperformed or matched currently used strategies in terms of sensitivity, specificity, and precision. We validated the performance of the assays measuring total immunoglobulin G (IgG) levels; antibodies against severe acute respiratory syndrome coronavirus (SARS-CoV) or Middle Eastern respiratory syndrome (MERS)-CoV spike (S) protein; and SARS-CoV-2 S and nucleocapsid (N) proteins and applied it to several large sample sets and real-world applications. We further established a TR-FRET-based ACE2-S competition assay to assess the neutralization propensity of the antibodies. Overall, these TR-FRET-based serological assays can be rapidly extended to other antigens and are compatible with commonly used plate readers.

## INTRODUCTION

The ability to quantitatively measure the immune response to host or pathogen antigens is a crucial diagnostic tool in public health. The need to rapidly adapt and establish high-throughput testing centers became especially evident at the onset of the COVID-19 pandemic caused by the severe acute respiratory syndrome coronavirus 2 (SARS-CoV-2).[1] While nucleic acid-based tests for the identification of infected individuals were rapidly and widely implemented,[2] these tests can only detect the virus during a narrow window of acute disease. Robust serological assays are necessary to identify individuals who have previously been infected or are asymptomatic and developed antibodies to SARS-CoV-2.[3,4] More broadly speaking, serological testing can also help epidemiologists to accurately model the prevalence of infections by establishing the spread of a virus within a population. Once the vaccine for a given virus is available, serological testing can be employed to measure both disease- and vaccine-acquired immunity across variants of concerns.[5] Furthermore, serological testing is becoming an integral part of research studies in oncology and hospital settings.[6,7] Therefore, robust, user-friendly, and accurate serological assays are of critical importance.

The serological assays most widely used to detect viral antibodies, including anti-SARS-CoV-2, are enzyme-linked immunosorbent assays (ELISAs), quantitative suspension array technology (qSAT), and flow cytometry-based or commercial solutions on large diagnostics platforms.[3,8–22] However, these platforms have several critical limitations.[23–27] ELISAs suffer from limited scalability, primarily due to multi-step protocols with extensive wash steps that lead to the need for specialized equipment and automation. Other available assays are either not quantitative or require specialized analytical laboratory platforms that are not widely available. Homogeneous assay formats, such as split NanoLuc luciferase[28–30] antibody detection systems, present an attractive alternative but still require large-scale testing.

Recently, time-resolved Förster resonance energy transfer (TR-FRET) assays, which can be performed in homogeneous format without wash steps, have been proposed as an alternative. TR-FRET assays rely on a proximity-driven FRET transfer between a donor fluorophore (such as terbium [Tb]) and an acceptor fluorophore (such as BODIPY FL). Early proof-of-concept studies showed the utility of using TR-FRET assays for the detection of antibodies in *Brucella* infection,[31] and preliminary studies indicated that they could potentially be useful for the detection of SARS-CoV-2 antibodies in human serum as well,[32] for the detection of nucleocapsid (N) protein antigen,[28] or for assessment of ACE2-spike (S)-receptor-binding domain (RBD) competition.[33] However, large-scale evaluation of the technology has not been conducted. To broadly evaluate the technology, we established a large-scale TR-FRET-based test for the detection of SARS-CoV-2 immunoglobulin G (IgG)-type antibody levels against S protein or N protein in diverse serological samples and compared it with state-of-the-art ELISAs. In addition, we have also developed a TR-FRET assay for the detection of total IgG protein levels that performs on par to clinical tests. We have further established SARS-CoV or Middle Eastern respiratory syndrome (MERS)-CoV S protein IgG antibody detection assays using commercially available S protein reagents showing the versatility of the approach. Given that serological samples frequently include stabilizing agents and metal chelating agents such as EDTA, which may interfere with Tb-chelate, we employed CoraFluors, a series of serum-/plasma-stable luminescent Tb complexes that mitigate these limitations.[34] Through testing diverse sample sets across 1,519 total samples, we demonstrated that the assay performs on par with commercial and academic tests that have previously been evaluated on the same sample sets while reducing both the processing time and the cost per sample. The minimal sample requirement (<1 μL plasma/serum) also enables more accessible sample collection protocols such as finger prick capillary instead of blood draws. The removal of wash steps and simplified sample handling increased reproducibility and repeatability (coefficient of variation [CV] < 5%), and will enable future implementation without the need for automated sample handling. Beyond antibody detection, we further demonstrated that the TR-FRET testing platform is extensible to new applications by implementing a rapid surrogate ACE2 neutralization assay.

## RESULTS

### Development of a TR-FRET assay to detect SARS-CoV-2 antibodies

We developed and validated a homogeneous serological assay platform for the detection of SARS-CoV-2 antibodies in human plasma/serum (Figure 1A). The direct detection of a ternary complex between antigen and serum antibodies using a TR-FRET readout allowed for a simple mix-and-read protocol that lends itself to scalable automation (Figures 1B and S1A–S1D). The proximity of the donor (CoraFluor-1) and acceptor (BODIPY FL) fluorophores induced by the presence of serum antibodies resulted in a positive TR-FRET signal that is read out as a 520 (acceptor)/490 nm (donor) ratio and allowed for accurate quantification of serum antibodies in an isotype-specific manner (Figure 1A).

To enable sensitive detection, we optimized assay conditions to minimize the signal-to-noise ratio. We first established that the TR-FRET assay format could detect the binding of Ig variants IgG, IgM, and IgA1 to SARS-CoV-2 antigens (Figure 1C). The SARS-CoV-2 S protein is responsible for binding to the host receptor ACE2 to mediate virus entry upon infection[35] and most neutralizing antibodies have been found to target the S protein.[36] We therefore used S protein and the RBD of the SARS-CoV-2 S protein (S-RBD) for assay development. S protein and S-RBD, expressed and purified from Chinese hamster ovarian (CHO) cells, were labeled with CoraFluor-1 or BODIPY FL (see STAR Methods). Detection antibodies (αIgG, αIgM, αIgA1) were commercially obtained and labeled with either CoraFluor-1 or BODIPY FL. As positive control, we used the recombinantly expressed SARS-1 IgG antibody CR3022,[37] which has been shown to cross-react with the S-RBD of SARS-CoV-2 ($K_d \leq 9.1 \pm 0.7$ nM; Figure S1E), and IgM and IgA1 antibodies engineered to contain the CR3022 variable region.[38] To identify ideal labeling positions, titrations of CR3022 (IgG, IgM, IgA1) into a mix of labeled S-RBDs and labeled detection antibody were performed while varying the position of donor and acceptor (either on the S-RBD or detection antibody) (Figures S1F and S1G). While we found that all

CellPress
OPEN ACCESS

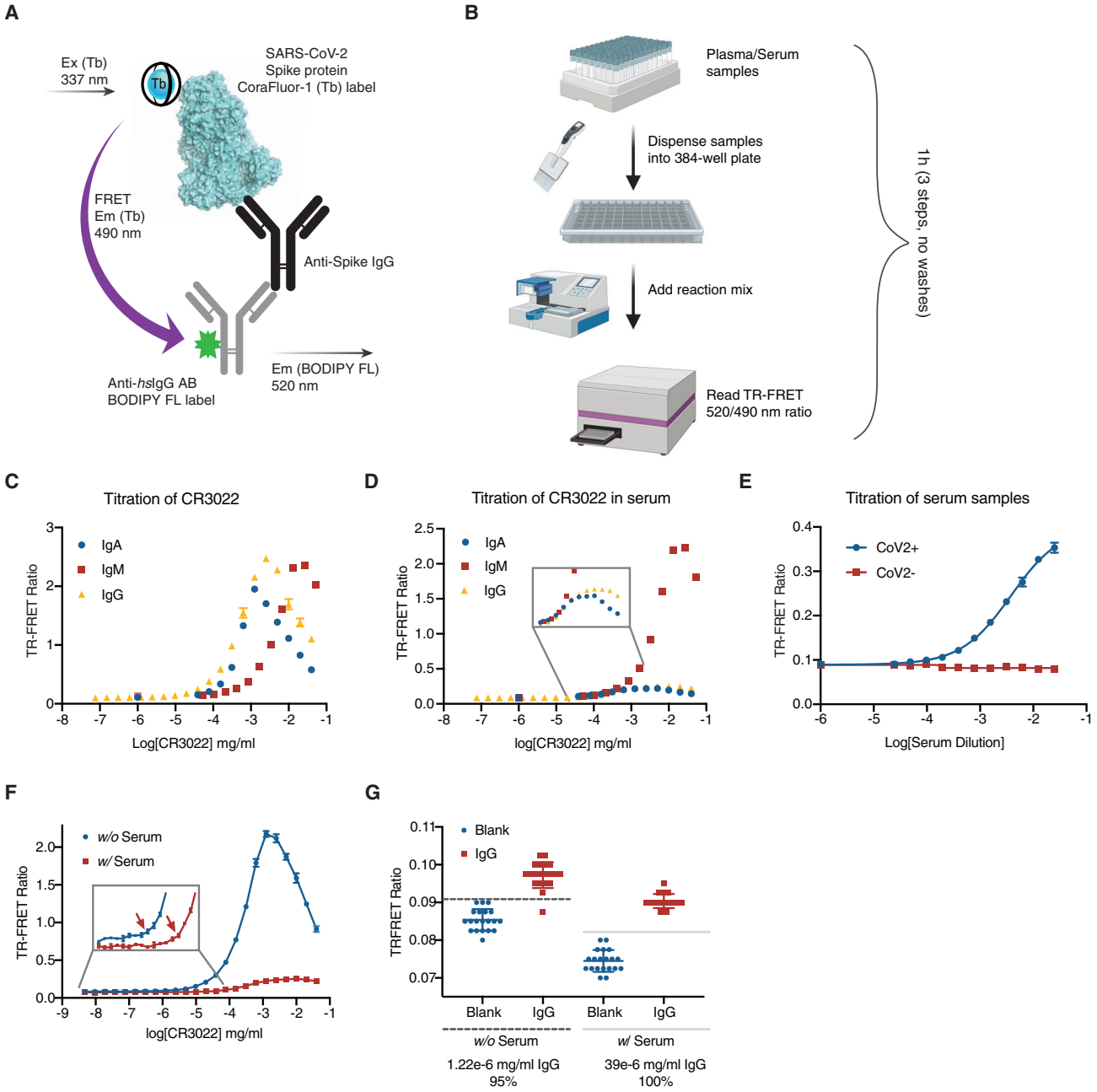


**Figure 1. TR-FRET assay setup, flowchart, and validation by CR3022 antibody**

(A) Principle of TR-FRET assay. Antibodies recognizing human IgG were labeled with BODIPY FL. SARS-CoV-2 S proteins were labeled with CoraFluor-1 (Tb) and were both mixed with serum for isotype-specific antibody detection. The light pulse at 337 nm excites the CoraFluor-1 (Tb)-labeled S protein and emits light at 490 nm, which in turn triggers energy transfer to the BODIPY FL-labeled secondary antibodies found in proximity induced by the analyte generating a TR-FRET signal detected at 520 nm.

(B) Flowchart of TR-FRET assay. The serum samples are diluted into microtiter plates and added into reaction mixture. Reaction mixture is added beforehand by an automated dispenser (Multidrop Combi Reagent Dispenser). The diluted serum samples are added into the reaction mixture using a Gryphon (Art Robbins Instruments) or manually by multi-channel pipetting. Plates are read on a TR-FRET-compatible plate reader (e.g., PHERAstar FSX Microplate Reader).

(C) Titration of CR3022 IgG/IgM/IgA1 into pre-formed mix of Tb-S protein (7.5 nM final) and BODIPY FL-labeled αIgG/αIgM/αIgA (250 nM final).

(D) As in (C) but in the presence of 1:150 dilution of negative serum.

Data of (C) and (D) are represented as means ± SD of two technical replicates (n = 2).

(E) Titration of positive and negative serum in final assay condition 250 nM BODIPY FL-αIgG and 7.5 nM Tb-S. Data are represented as means ± SD of three technical replicates (n = 3).

*(legend continued on next page)*

combinations lead to a functional readout (Figures S1H and S1I), we observed that donor conjugation to the antigen results in optimal performance when used with serum samples (Figures S1K and S1L). We therefore selected labeling the antigen with CoraFluor-1 and the detection antibody with BODIPY FL, resulting in quantitative binding curves for CR3022 (IgG/IgM/IgA1) (Figure 1C). The binding curves exhibited a characteristic bell shape due to the prozone effect,[39] whereby analyte levels, in this case IgG, are high and saturate both S protein and BODIPY FL-anti-IgG antibody, resulting in binary complexes rather than a productive ternary complex. These effects can be accurately accounted for by mathematical models.[40] We next established that CR3022 can similarly be detected in human serum (Figure 1D), and while the signal is reduced, the low background level allows for accurate quantification. During the optimization of assay conditions, we noticed that replacing the RBD with the full-length SARS-CoV-2 S protein significantly reduced background, particularly in the presence of serum. This is likely due to (1) the trimeric nature of the full-length S protein leading to avidity effects and (2) the exposure of otherwise shielded RBD surfaces that may cause unspecific interactions. We therefore continued all further validation using S protein and subsequently optimized the concentrations of antigen and detection antibody (Figures S2A and S2B). With optimized concentrations (250 nM BODIPY FL-anti-IgG, 7.5 nM Tb-S), we validated that convalescent serum results in a dose-dependent response in TR-FRET signal (Figure 1E) as well as confirmed that the prozone effect is not affecting the readout at the final serum concentration of 1:150 (v/v) (Figure S1J).

## Analytical limit of detection

To assess the limit of detection (LoD) of the TR-FRET assay, we first performed a titration of control antibody CR3022 IgG in the presence and absence of negative control serum at 1:150 serum to buffer dilution (Figure 1F). The prozone effect was clearly visible at higher concentrations of the antibody, and signal intensity was reduced in the presence of serum. We next selected the lowest concentrations of CR3022 IgG antibody where the signal was higher than mean + 3 standard deviations (SDs) and compared 20 replicates against the 20 replicates of blank control both in the presence and absence of serum (Figure 1G). Based on this, the LoD for the TR-FRET assay was determined to be 1.22 ng/mL in the absence of serum and 39 ng/mL in the presence of serum, which is in the range of common ELISA LoDs.[41]

## Homogeneous TR-FRET assay can detect IgG in patient serum

To test the detection of antibodies in serum obtained from positive and negative controls, a set of 48 PCR-tested-positive (CoV2+) patients from Mass General Hospital (MGH) and Brigham and Women's Hospital (BWH) and 28 PCR-tested-negative (healthy, CoV2−) patients from MGH, as well as 19 pre-pandemic serum samples from Mass General Brigham Biobank (CoV2−) or community volunteers (CoV2−), was assembled (hereafter referred to as 96w_testset) (Table S1). Adapting established protocols,[42] we performed an ELISA using S protein as reference (Figure S2C). We next profiled the 96w_testset with our TR-FRET assay at an initial serum dilution of 1:100 to match the exact ELISA concentration (Figure S2D) and found that when using a 3 SD cutoff away from the healthy control mean, the TR-FRET achieved comparable sensitivity and slightly improved specificity compared with the ELISA results (Figures S2C and S2D). We note that the 96w_testset was collected during the first weeks of the pandemic and may contain false negatives and therefore was not used to formally establish assay performance but rather served for optimization. We observed a strong correlation between the TR-FRET assay and ELISAs (Figure S2E). While the discrimination between CoV2+ and CoV2− was comparable between TR-FRET and ELISA, we found that the ELISA had a stronger signal compared with TR-FRET for low responders. This can be explained by the signal amplification in the ELISA compared with equilibrium binding of the TR-FRET assay. However, the lower signal was offset by the low background noise of the TR-FRET, and additionally, the TR-FRET had a larger dynamic range without the ceiling of signal at higher antibody concentrations seen with ELISA (Figure S2E). Nevertheless, we wondered whether the signal could further be boosted without compromising background noise by increasing the serum concentration and how the assay would react to changes in serum dilution. We re-assayed the 96w_testset using dilution factors of 1:150 or 1:50 and observed that increasing the serum concentration improves signal strength without compromising background noise (Figures S2F–S2I). Lowering the serum concentration to 1:150 only marginally reduced performance (Figure S2H). When analyzing this initial 96w_testset, we observed several CoV2+ samples with unexpected low response. In addition to the above-mentioned limitations of the 96w_testset, we hypothesized that this might be the result of epitope masking since the TR-FRET assay utilizes covalent labeling of the antigen with CoraFluor-1. We therefore sought to ensure minimal epitope masking and optimized the degree of labeling (DOL) (Figures S3A and S3B). We found that a DOL ~3.8 resulted in no detectable epitope masking with an optimal signal, and therefore a DOL ~3.8 was ensured for all further validation experiments. The measured DOL of the BODIPY FL-anti-IgG was 2.7.

## TR-FRET assay can accurately detect seroconversion

With optimized conditions and DOLs, we next used the TR-FRET assay to detect seroconversion in a larger set of samples from the Mass General Brigham Biobank containing 68 SARS-CoV-2 PCR-positive samples (CoV2+) and 100 pre-pandemic healthy controls (healthy, CoV2−) (hereafter referred to as MGB set; see Table S1) that was again profiled using the established ELISA for reference and has also been profiled with different commercial and academic assays.[43] In line with our previous observations, the SD of the healthy controls was very

(F) TR-FRET αIgG-S assay. Titration of CR3022 IgG in the presence and absence of negative serum at 1:100 dilution. Data are represented as means ± SD of three technical replicates (n = 3). The concentration of CR3022 selected for the LoD study is highlighted with a red arrow.
(G) TR-FRET αIgG-S. LoD for TR-FRET assay was assessed by comparing 20 replicates of the CR3022 with 20 replicates of buffer control in the presence and absence of negative serum at 1:100 dilution.

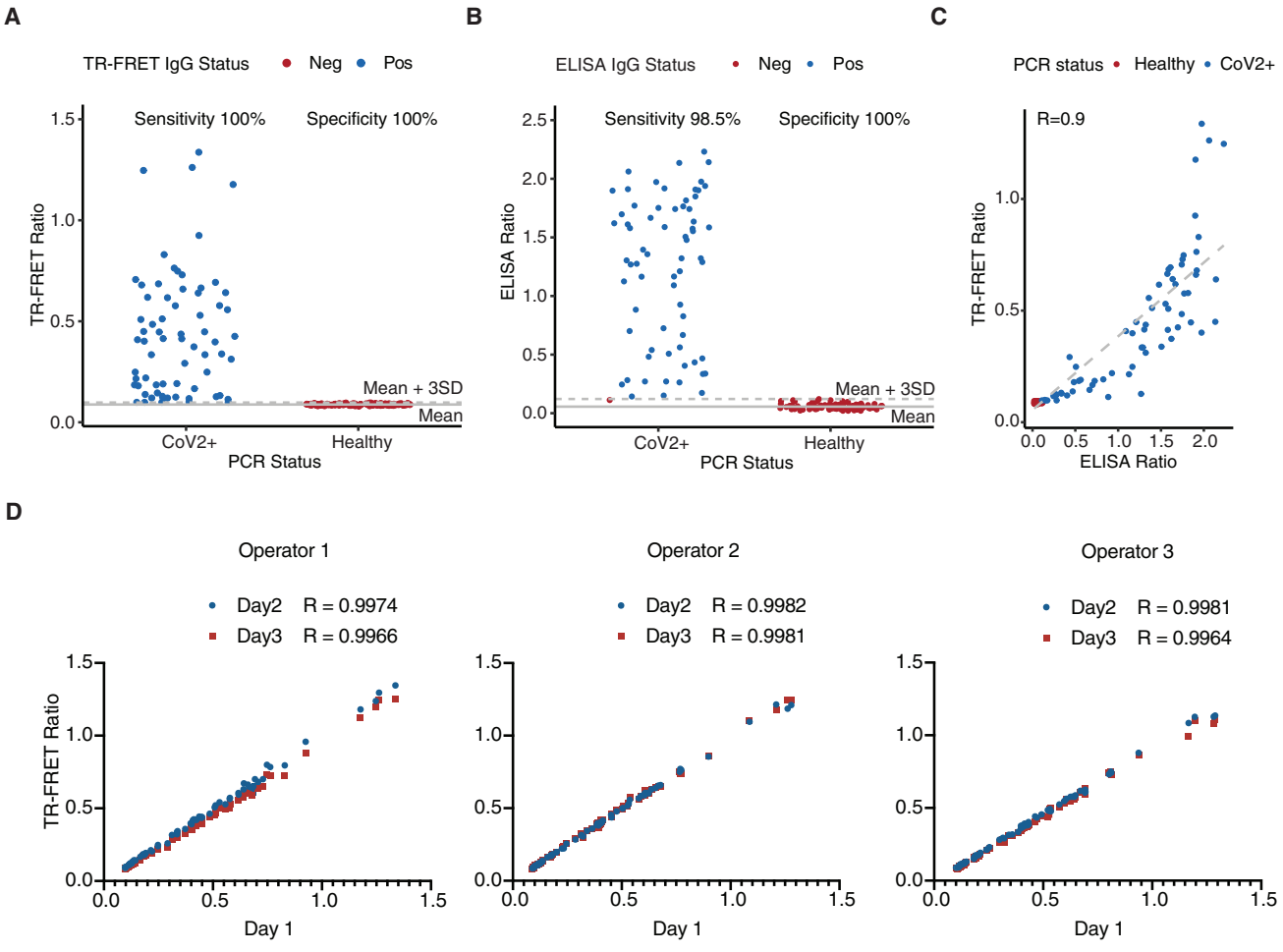


E

| | Average Repeatability across operators | Average Intermediate precision across days and operators |
|---|---|---|
| IgG | 4.31 | 5.79 |

**Figure 2. Performance of TR-FRET assay: Sensitivity, specificity, and precision**

(A) Sensitivity and specificity of ELISA IgG assay performed on a cohort of 68 SARS-CoV-2 PCR-positive samples (CoV2+) and 100 pre-pandemic negative samples (healthy).

(B) Sensitivity and specificity of TR-FRET αIgG-S performed on the same cohort.

(C) Correlation of TR-FRET IgG with serum dilution 1:150 and ELISA IgG at serum dilution 1:100. Data are represented as means ± SD of two technical replicates (n = 2).

(D) Comparison between three independent runs performed on different days by three different operators of a TR-FRET αIgG-S assay on a set of positive responders as well as negative control samples (68 total).

(E) The calculated average repeatability across operators (CV%) and average intermediate precision (calculated across days and operators) corresponding to data in (D). Data are represented as means ± SD of two technical replicates (n = 2).

low, and accurate discrimination between CoV2+ and healthy samples was achieved with 100% specificity and 100% sensitivity using a cutoff based on 3 SDs of the healthy control (Figure 2A). The results were comparable to the established ELISA on the same sample set (Figure 2B), and the response of individual samples between TR-FRET and ELISAs was well correlated (Pearson correlation coefficient of 0.9) (Figure 2C), again showing an increased dynamic range for the TR-FRET assay as opposed to the ELISA. The MGB set contained samples from patients of ages between 30 and 70 years for the CoV2+ cohort and between 20 and 70 years in CoV2− group (Figure S2J). The gender distribution was 35 female and 33 male samples in the CoV2+ cohort and 30 female and 70 male samples in the pre-pandemic healthy control group (Figure S2K). While we noticed that the IgG titers against S antigen were higher in the younger age group (30s), the significant variability of the

IgG levels indicated diverse responses within the tested population (Figure S2L).

### Assessing intra- and inter-assay precision for the TR-FRET assay

Eliminating the need for wash steps and reducing the overall number of sample handling steps should result in high reproducibility and repeatability. To assess the intra- and inter-assay precision of the TR-FRET assay, we selected a set of positive responders as well as negative control samples (68 total) and performed the assay with three operators on three different days (Figures 2D and 2E). The correlation between operators was above 99.6% with an average repeatability of 4.31% and an overall precision across days and operators of 5.72%, which well exceeds the commonly desired range for serological assays.[44]

### TR-FRET assay can rapidly be extended to additional antigens

Having established a serological assay for the S protein, we set out to assess whether the TR-FRET setup is compatible with other antigens. S protein and S-RBD are the most widely used antigens in serological assays for SARS-CoV-2, but there are other SARS-CoV-2 proteins that are highly immunogenic,[45] such as the abundant N protein, which binds to viral RNA inside the virion.[46,47] We established an N protein TR-FRET IgG detection assay (hereafter named N TR-FRET) utilizing the same TR-FRET setup as before, with the donor fluorophore on the antigen and the acceptor fluorophore on the αIgG antibody. The N protein was expressed from insect cells and biotinylated, and CoraFluor-1-streptavidin (Tb-SA) conjugate was used to label the antigen. To validate the assay setup, we performed a titration of convalescent CoV2+ serum into biotinylated N protein, Tb-SA, and BODIPY FL-αIgG. We observed a dose response with strong signal present at a dilution of 1:150, consistent with our S protein TR-FRET (Figure S3C). We next performed N TR-FRET on the 96w_testset, which resulted in a sensitivity of 80% and specificity of 96.6% (Figure S3D).

To further assess performance of the established IgG S and N TR-FRET assays, we utilized a larger sample set from the MassCPR consortium with 100 SARS-CoV-2 RT-PCR-positive samples (CoV2+), as well as 90 pre-pandemic controls from the Dana-Faber Cancer Institute Bio Bank (heathy), hereafter named the MassCPR set (Table S1). Using the established mean (healthy) + 3 SD (healthy) cutoff, the TR-FRET assay performance was established with 97.1% sensitivity and 97.8% specificity, respectively, for the S antigen and 95.2% sensitivity and 98.9% specificity, respectively, for the N antigen (Figures 3A and 3B). The analogous results using the ELISA resulted in 95.2% sensitivity and 97.8% specificity for the S antigen and 94.3% sensitivity and 98.9% specificity for the N antigen (Figures S3F and S3G). In both S and N assays, TR-FRET showed improved sensitivity over ELISA (97.1% for S TR-FRET, 95.2% for S ELISA, 95.2% for N TR-FRET, and 94.3% for N ELISA) with identical specificity. As seen before with the MGB set, we noticed a "ceiling" of signal with the ELISA readout and an increased dynamic range for the TR-FRET assay (Figures 3C and 3D). The clinical admission status of the MassCPR sample cohort indicated that 19 patients were admitted to the emergency room (ER), 76 were admitted as inpatients (IPs), and 5 were admitted as outpatients (OPs). We did not observe a significant difference in the IgG S antibody titers between the groups (Figure S3H). The number of days since the last positive SARS-CoV-2 test was recorded, and within the 14–30 day period, IgG levels varied without significant trends (Figure S3I), in line with previously reported longitudinal studies where the S IgG level stabilizes 14 days post infection.[48] Comparing the S and N TR-FRET readouts on the MassCPR and 96w_testset resulted in a Pearson correlation coefficient of 0.37 for the 96w_testset (Figure S3E) and 0.22 for MassCPR (Figure 3E), indicating that the two assays are partially orthogonal and likely provide additive information on serological status when combined, which is in accordance with what has been found in other studies[49] (Figures 3E and S3E). The S protein has high sequence similarity between SARS-CoV-2, SARS-CoV, and, to lesser extent, MERS-CoV, which can result in cross-reactivity in the antibody response.[50–52] In analogous fashion to the SARS-CoV-2 S TR-FRET assay, we have established S-based IgG detection assays for SARS-CoV and MERS-CoV and tested the MassCPR set of samples. As expected, we observed cross-reactivity between SARS-CoV-2 and SARS-CoV (Figure 3F) but very limited cross-reactivity with MERS-CoV (Figure 3G). This, again, is in line with previous observations using these antigens and demonstrates that the TR-FRET assay behaves similar to ELISA and other formats and that cross-reactivity or sensitivity are largely determined by the choice of antigen.[53] Interestingly, we have identified samples with a high titer of IgG antibodies against MERS-CoV S in ~6% of CoV2+ samples tested.

### TR-FRET assay is compatible with diverse sample types

A useful and robust diagnostics platform needs to be rapidly deployable and capable of being modified to varying needs. This also often includes a requirement for handling diverse sampling methods that are determined by access to the targeted cohort. Specifically, self-collection is an important tool for field studies or sample collection in remote locations, and we therefore explored the performance of TR-FRET-based serology using self-collection of whole dried blood samples using Neotheryx kits in a controlled manner by having paired serum samples within a short time interval of each other. Strikingly, we observed that the TR-FRET assay exhibits low variability of the background signal across both serum and whole-blood sample types (Neotheryx), while for ELISA measurements, the background significantly increases in variability for the whole-blood sample (Figure 4). The increased background noise in the hemolyzed samples led to reduced signal to noise and Z′ in the ELISA, while the performance of the TR-FRET assay was not altered (Figure S4). This study demonstrates how this assay can perform in circumstances where other research tests fail. In this specific case, the whole dried blood samples led to a very high background in ELISA-type assays, while the TR-FRET readout, as an "in solution" assay, is unaffected.

### Limitation of TR-FRET assay for samples with high IgG levels

To obtain robust validation of the IgG-S TR-FRET assay, we have profiled a large cohort of hematologic malignancies

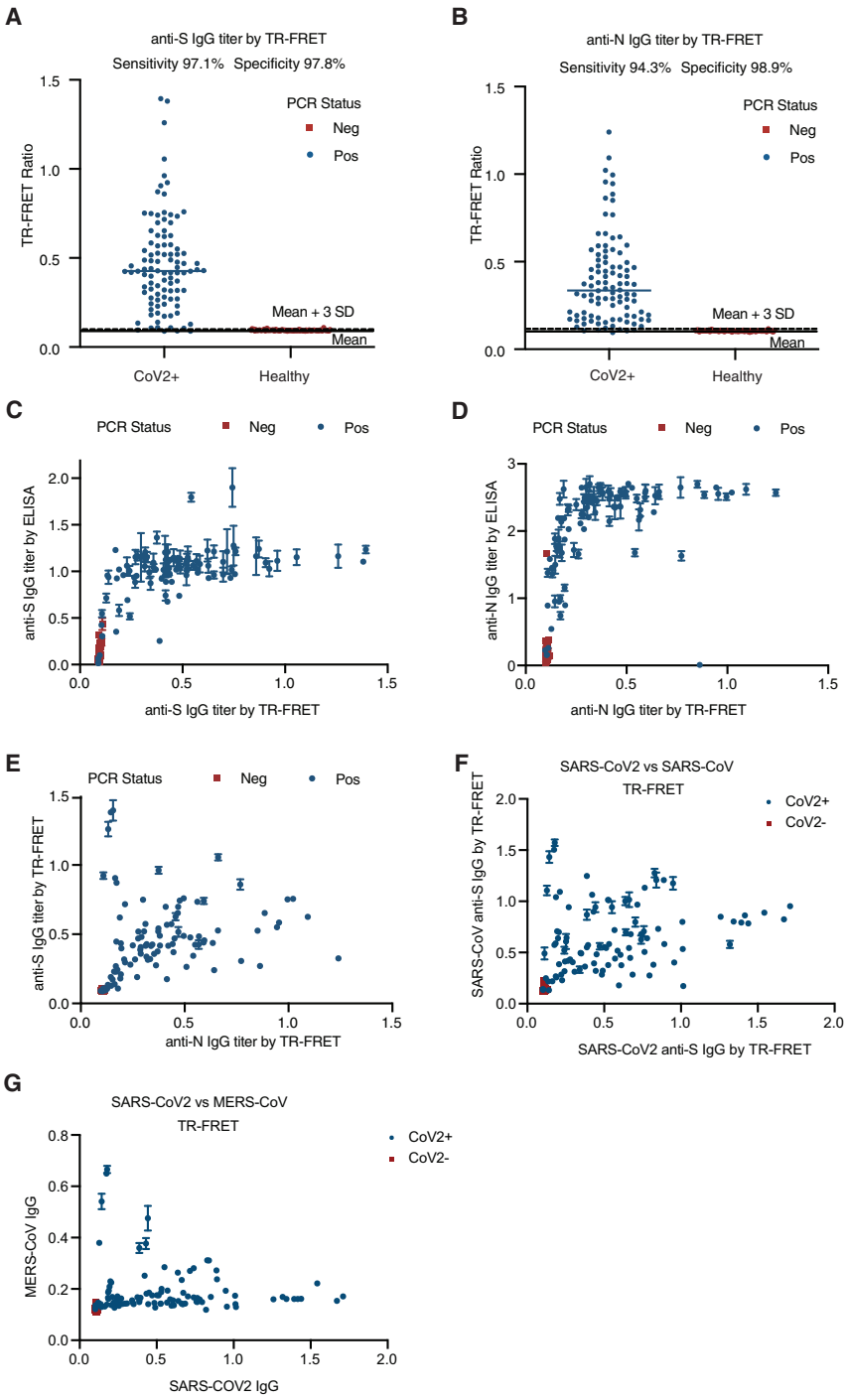


**Figure 3. TR-FRET assay format is compatible with other antigens**

(A) Sensitivity and specificity of TR-FRET αIgG-S protein assay performed on MassCPR set including 90 pre-pandemic negative samples and 100 SARS-CoV-2-positive samples.

(B) Sensitivity and specificity of TR-FRET αIgG-N protein assay performed on MassCPR.

(C) Correlation of αIgG-S titer in TR-FRET assay versus ELISA for MassCPR. Note the "ceiling" of the signal in ELISA and the high dynamic range of TR-FRET.

(D) Correlation of IgG titer N protein in TR-FRET assay versus ELISA for MassCPR.

(E) Correlation of TR-FRET αIgG-S and TR-FRET αIgG-N assays performed on MassCPR indicates diverse immune response to different antigens.

(F) Cross-reactivity between S proteins of SARS-CoV-2 and SARS-CoV measured by TR-FRET IgG titer on MassCPR.

(G) As in (F) but for S proteins of SARS-CoV-2 and MERS-CoV.

Data are represented as means ± SD of two technical replicates (n = 2).

(multiple myeloma and Waldenstrom macroglobulinemia) patient samples from the IMPACT study (DFCI IRB #20-332), which showed reduced serological response to COVID-19 vaccines.[6] Patients with these B cell cancers frequently exhibit abnormal total Ig levels. We observed good correlation between ELISA IgG-S with TR-FRET IgG-S (Figure 5A) for the majority of samples; however, we noticed that for samples with total IgG concentrations higher than 2,500 mg/dL, the TR-FRET IgG-S values were reduced compared with the ELISA IgG-S (Figures 5B–5D). We noted that the IMPACT study sample patients exhibited high IgG concentrations (Figure 5E); therefore, given that antigen was not immobilized in our TR-FRET assay format, the BODIPY FL-labeled secondary IgG antibodies could bind to all IgG antibodies reducing total signal, explaining the TR-FRET results under high IgG concentrations conditions. We confirmed that interference by the non-specific IgG is only observed at >2,500 mg/dL total IgG. In a typical healthy cohort, IgG ranges between 400 and 2,170 mg/dL,[54] and TR-FRET assay performance was not affected. To be able to classify patients with high total IgG levels, we have developed a rapid TR-FRET-based total IgG detection assay (Figures 5F, 5G, and S5A). In this format, protein G labeled with CoraFluor-1 is the TR-FRET donor and anti-IgG NanoBody (CTK0101, Nano-Secondary, ChromoTek) labeled with AF488 is the TR-FRET acceptor. We determined that the TR-FRET total IgG assay with the 1:40,960 dilution of serum gave the best correlation with ELISA total IgG with $R^2$ of 0.908 (Figures 5H and S5B–S5F).

## TR-FRET ACE2-S assay detects neutralizing antibodies

A limitation of antibody detection assays such as ELISA or the TR-FRET test developed here is that they do not discriminate antibodies based on their ability to neutralize the virus. The

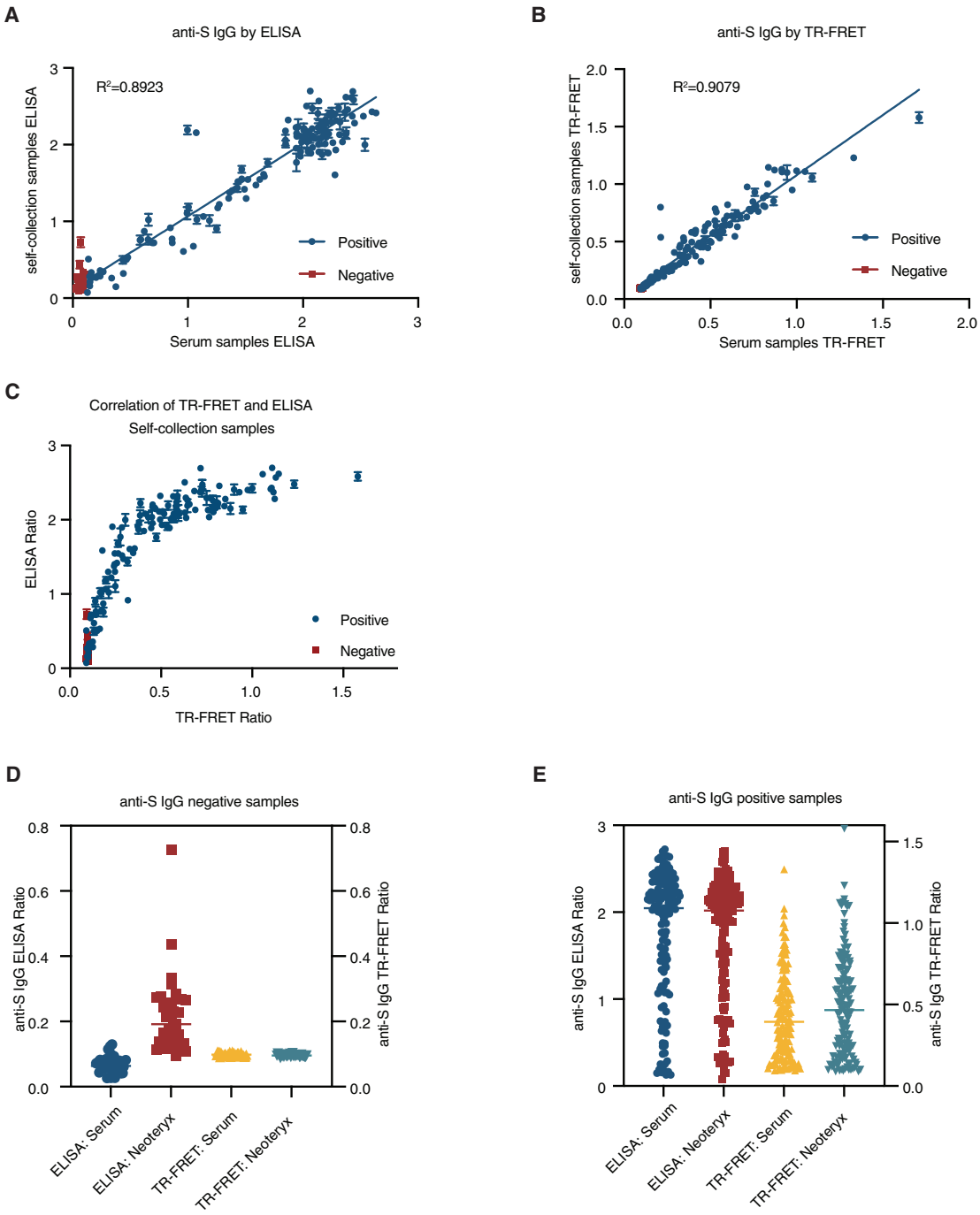


**Figure 4. TR-FRET assay accepts multiple sample types**

(A) Correlation of ELISA IgG-S response between the matched set of whole dried blood self-collection samples (Neotheryx kit) and serum samples from the same donors collected within 2 weeks of each other at the Dana-Farber Cancer Institute (DFCI; IRB #20-260).

(B) As in (A) but for TR-FRET IgG-S assay.

(C) Correlation between TR-FRET and ELISA responses in the IgG-S assay on the self-collection samples.

(D) The response of ELISA or TR-FRET assay compared between a set of SARS-CoV-2 negative samples.

(E) The response of ELISA or TR-FRET assay compared between a set of SARS-CoV-2 positive samples.

Data are represented as means ± SD of two technical replicates (n = 2) on a cohort of 140 CoV2+ and 35 CoV2 samples.

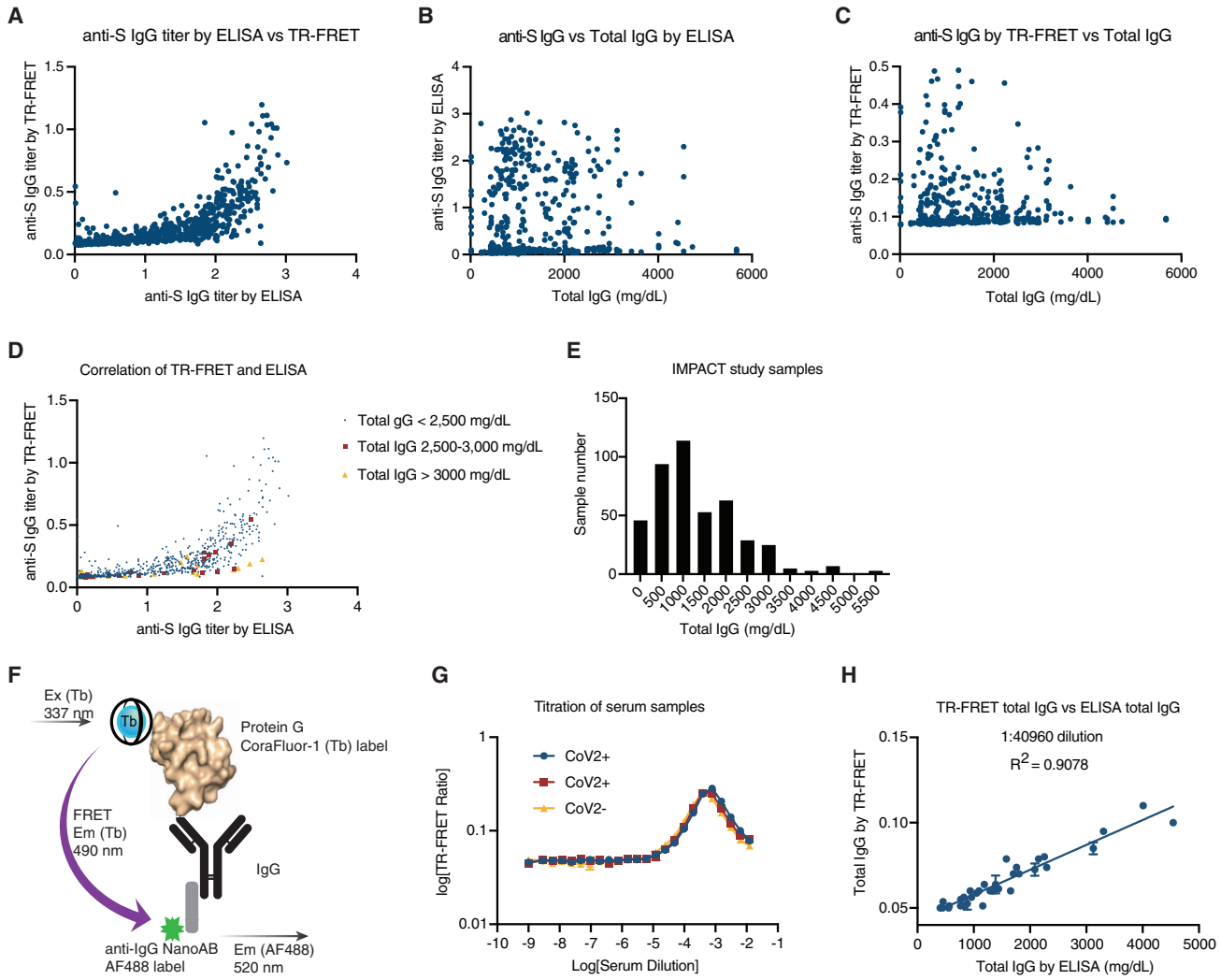


**Figure 5. TR-FRET can be applied for total IgG amount testing and validation**

(A) Correlation between TR-FRET and ELISA responses in the IgG-S assay on IMPACT study samples.

(B) Correlation between ELISA in the IgG-S assay and total IgG on IMPACT study samples.

(C) Correlation between TR-FRET in the IgG-S assay and total IgG on IMPACT study samples.

(D) Correlation of ELISA and TR-FRET with total IgG with difference total IgG levels. Total IgG <2,500 mg/dL is labeled as blue. Total IgG in the range 2,500–3,000 mg/dL is labeled as red. Total IgG >2,500 mg/dL is labeled as yellow.

(E) Histogram of total IgG levels in the IMPACT study.

(F) The principle of TR-FRET total IgG assay. Nanobodies recognizing human IgG are labeled with AF488. Immunoglobulin-binding protein G is labeled with Tb (terbium). The light pulse at 337 nm excites Tb chelate protein G and emits light at 490 nm, which in turn triggers energy transfer to AF488-labeled nanobodies found in proximity induced by the analyte generating a TR-FRET signal detected at 520 nm.

(G) Titration of positive and negative serum in final assay condition 25 nM Tb-protein G and 25 nM AF488-nanobody. Data are represented as means ± SD of two technical replicates (n = 2).

(H) Correlation of total IgG measured by TR-FRET and ELISA on a set of 39 samples at 1:40,960 dilutions. Data are presented as n = 1 for ELISA and as two technical replicates (n = 2) for TR-FRET.

detection of neutralizing antibodies (nAbs) is commonly conducted using either live SARS-CoV-2 virus assays (requiring BSL3 labs) or pseudotype virus assays (requiring BSL2 labs), which are both limited in throughput and availability.[55,56] Since the dominant neutralizing mechanism for SARS-CoV-2 is to block binding between the SARS-CoV-2 S protein and the human ACE2 receptor, we hypothesized that this interaction can be leveraged to build a surrogate neutralization assay and that such a test should be similarly rapid, scalable, and easy to implement (Figure 6A). To test this, we first established that our TR-FRET readout can accurately detect and quantify binding between BODIPY FL-labeled S protein (BODIPY FL-S) and biotinylated recombinant human ACE2 (btn-ACE2) in the presence of CoraFluor-1-labeled SA (Tb-SA) (Figure S6A). To establish whether the assay can accurately detect the presence of nAbs, we next titrated increasing concentrations of four

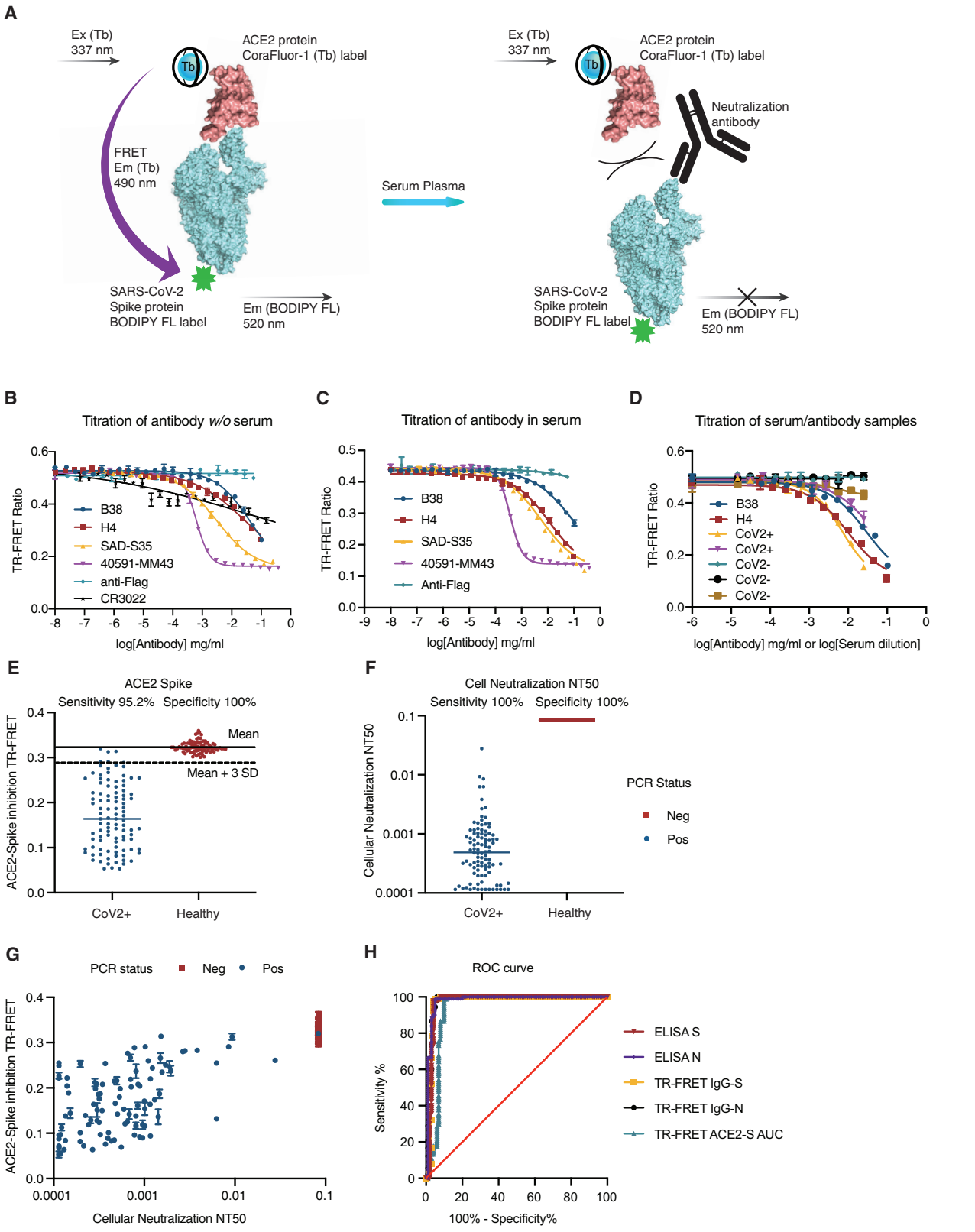


(legend on next page)

well-characterized recombinant human and mouse nABs targeting the S protein (B38,[57] H4,[57] SAD-S35 [Acro Biosystems, Newark, DE, USA], and 40491-MM43 [Sino Biological, Beijing, China]), the S protein-binding but non-nAb CR3022, and a non-binding control antibody (see STAR Methods for details) to btn-ACE2 (at 8 nM), BODIPY FL-S (at 8 nM), and Tb-SA (at 2 nM). In agreement with the literature-reported efficacies, all four nAbs were able to effectively compete with the ACE2-S interaction and scored as neutralizing in our assay both in the presence of buffer (Figure 6B) or serum (Figure 6C). Consistent with these findings, titration of either negative (pre-pandemic control) or positive (CoV2+, PCR and IgG positive) patient sera resulted in a dose-dependent signal only for the CoV+ serum (Figure 6D, B38 and H4 nAbs included for reference). We also assessed the robustness of the assay setup, and similar to the TR-FRET serological assay, the ACE2-S assay tolerated different labeling strategies such as btn-ACE2 with Tb-SA or direct labeling of ACE2 with CoraFluor-1 (Tb-ACE2) combined with various concentrations of BODIPY FL-S (Figures S6B–S6F).

### TR-FRET neutralization assay discriminates CoV2+ patient samples

Having established that the TR-FRET ACE2-S assay can accurately detect the ability of recombinant purified antibodies to compete with the interaction critical for viral infection, as well as in patient sera, we next sought to determine the performance of this assay to discriminate CoV2+ patient serum samples from healthy individuals. Using the 96w_testset and the MassCPR set (described above), we profiled these samples in the TR-FRET ACE2-S assay for neutralizing activity (Figures 6, S6, and S7). While none of the healthy control samples exhibited any detectable neutralizing activity, most of the CoV2+ samples had varying levels of neutralizing activity (Figure 6E). We also assessed the neutralization status of the MassCPR set in a cellular pseudovirus neutralization assay[58] (Figure 6F). The response of the TR-FRET ACE2-S inhibition as measured by the TR-FRET value (Figure 6G) or area under the curve (AUC) (Figures S7A and S7B) was correlated with the NT50 values reported by the cellular neutralization assay. In line with what has been observed with pseudotype virus assays[58] and other surrogate neutralization assays,[59,60] we observed a correlation of total S-specific IgG levels and neutralization activity of either the TR-FRET assay or the cellular neutralization assay (Figures S6G and S6H). A similar trend was also observed for the anti-N protein IgG antibody titers (Figures S6I and S6J). While the TR-FRET ACE2-S assay is, in principle, sensitive to neutralization by any serotype (IgM or IgA), the majority of activities in these samples appeared to result from IgG levels (Figure S7B). Importantly, we found that the neutralization assay by itself can successfully discriminate CoV2+ from healthy individuals in the 96w_testset cohort (Figure S7C) as well as in the MassCPR set (Figure 6E), consistent with what has been observed using other neutralization assays.[58] When receiver-operating characteristic (ROC) analysis was performed (Figures 6H and S7D), we found that the ACE2-S assay performed comparable to the TR-FRET and ELISA serological assays in discriminating CoV2+ patient samples from healthy control samples (Figures 2A, 2B, 6E, and S7C).

## DISCUSSION

We established a homogeneous serological assay platform based on TR-FRET detection using novel serum/plasma stable CoraFluor-1 TR-FRET donors, which provide a scalable alternative to current assay platforms. While assays with signal amplification such as ELISA,[16,17,61] or digitized detection such as SIMOA,[62] in theory offer superior detection at low levels of analyte, the TR-FRET assay described here offsets this by exhibiting low background, allowing for sensitive, accurate detection of SARS-CoV-2 seroconversion. The lack of signal amplification biases the assay toward superior specificity due to very stable background signal and results in robust reproducibility and repeatability (CV < 5%) along with an extended dynamic range compared with colorimetric ELISA, which was designed for high sensitivity. When compared with common commercial assays or ELISAs on the same samples,[43] the TR-FRET assay performed equivalently or superiorly in discriminating SARS-CoV-2.

As we demonstrate with the use of biotinylated N protein, as well as with SARS-CoV or MERS-CoV S protein, the TR-FRET assay setup offers a flexible platform for rapid onboarding of new antigens of the same pathogen and can also be easily

**Figure 6. TR-FRET neutralization assay setup and validation**

(A) Principle of TR-FRET neutralization assay. Human ACE2 receptor is labeled with CoraFluor-1. SARS-CoV-2 S protein is labeled with BODIPY FL, and both are mixed with serum for neutralization antibody detection. After excitation at 337 nm, emission at 490 (CoraFluor-1) and 520 nm (BODIPY FL) is detected, and the TR-FRET ratio is calculated as a 520/490 signal. Neutralizing antibodies present in the serum will competitively bind the S protein and reduce the TR-FRET signal.

(B) Titration of B38, H4, SAD-S35, 40491-MM43, CR3022, and a negative control αFLAG into pre-formed mix of btn-ACE2 (8 nM final), Tb-SA (2 nM final), and BODIPY FL-S (8 nM final). Data represented as means ± SD of two technical replicates (n = 2).

(C) As in (B) but performed in the presence of serum. Data represented as means ± SD of three technical replicates (n = 3).

(D) Titration of positive and negative serum in final assay condition 8 nM btn-ACE2, 2 nM Tb-SA, and 8 nM BODIPY FL-S. Data represented as means ± SD of two technical replicates (n = 2).

(E) Sensitivity and specificity of TR-FRET ACE2-S neutralization assay performed on MassCPR (90 pre-pandemic negative samples and 100 SARS-CoV-2-positive samples). Final serum dilution of 1:50 (v/v). Data represented as means ± SD of two technical replicates (n = 2).

(F) Sensitivity and specificity of reported cellular pseudovirus neutralization assay performed on MassCPR (90 pre-pandemic negative samples and 100 SARS-CoV-2-positive samples). Reported is the NT50, the concentration at which 50% of neutralization is observed as calculated from quadruplicate, 7-point dose response.

(G) Correlation of cellular neutralization NT50 against TR-FRET ACE2-S inhibition.

(H) Receiver-operating characteristic (ROC) curve indicating the performance of detection of IgG levels for S or N using ELISA or TR-FRET and TR-FRET ACE2-S inhibition assays.

All TR-FRET data in (E)–(H) are represented as means ± SD of two technical replicates (n = 2). ELISA data in (H) are represented as means ± SD of four technical replicates (n = 4).

adapted for testing other pathogens or analytes. Similar to the ELISAs,[5] the TR-FRET setup could be expanded to cover new variants of S or N proteins. We expect that the TR-FRET assay will be adaptable to find antibodies for other versions of the virus, such as Delta and Omicron, as it was able to detect antibodies for S proteins of SARS-CoV, MERS-CoV, and SARS-CoV2. The flexibility of an ''in solution'' detection will allow for future applications such as isotype-specific detection, multiple antigens in a single mix-and-read reaction, or the detection of specific epitopes. We demonstrate this flexibility by implementing a surrogate neutralization assay that accurately quantifies the ability of serum antibodies to interfere with the ACE2-S interaction, the primary mechanism of SARS-CoV-2 virus neutralization. These additional applications, as well as future applications, share the benefits of few sequential steps, enabling simple and robust scalability and automation.

Importantly, the TR-FRET serological assay performs robustly on difficult samples such as a cohort of self-collection dry-spot whole-blood samples. In contrast, the background signal of an ELISA increased in variability for a healthy patient sample set, likely affected by hemolysis, while the TR-FRET assay maintained high signal to noise, which did not compromise the detection (Figure S4). We find this result to be of high importance, as it demonstrates the robustness of the assay across multiple sample types. Furthermore, the ability to accurately process whole-blood spots could enable expansion to home-based serological testing schemes, significantly reducing barriers to obtaining samples and enabling the testing of individuals who otherwise would not be able to attend an in-person blood draw.

While our TR-FRET assay platform is versatile and can be easily adapted to new antigens (S, N, SARS-CoV S, and MERS-CoV S) and various sample types (serum as well as hemolyzed samples), our study identified limitations of the setup. When analyzing samples from a patient cohort with multiple myeloma, a plasma cell cancer that frequently results in abnormal Ig levels, we discovered that patients with high total IgG levels >2,500 mg/dL report lower TR-FRET responses (anti-S IgG) than expected by the ELISA S-IgG, resulting in the potential for false negatives in the TR-FRET assay. This effect is likely caused by the fact that the BODIPY FL IgG detection antibody binds to all available IgGs and that a high level of total IgG acts to dilute the specific BODIPY FL signal, resulting in reduced TR-FRET. To mitigate this issue, we established a nanobody-based TR-FRET total IgG detection assay, which maintains the simplicity of the protocol and can be used concurrently with the TR-FRET IgG-S method to identify problematic samples.

In conclusion, the TR-FRET assay platform fulfills an unmet need for a serological assay that is scalable and has a very low implementation barrier. The scalability arises from the lack of washing steps or sequential manipulations, enabling simple automation using widely available robotic platforms capable of a hundred thousand tests a day. The simplicity of the assay format also makes it easy to implement, and no automated plate washers or similar liquid handling systems are required, enabling reproducible results. With widely available plate readers, we have shown that one operator can perform several hundred tests a day using manual multi-channel pipettes without sacrificing the accuracy of the results. The TR-FRET-based serological tools have proven, in our hands, to be rapidly adaptable and robust methods that are now available as part of the pandemic response toolbox. We anticipate that the technology presented here and pioneered on samples of SARS-CoV-2 cohorts can be expanded for utility beyond viral infections, as represented here by our TR-FRET assay capable of measuring total IgG levels.

## Limitations of the study

The homogeneous TR-FRET assay setup can be limited by high total IgG concentration. Specifically, while testing the TR-FRET IgG-S setup on a cohort of myeloma patient samples (exhibiting high variability of total IgG levels), we noticed that high total IgG levels of more than 2,500 mg/dL reduce the TR-FRET signal compared with ELISA, which presents as a standing limitation for samples with high total IgG levels. To mitigate this issue, we have established a TR-FRET-based assay to measure total IgG levels that can be run concurrently with the IgG-S and allows for flagging of problematic samples.

## STAR★METHODS

Detailed methods are provided in the online version of this paper and include the following:

- KEY RESOURCES TABLE
- RESOURCE AVAILABILITY
  - Lead contact
  - Materials availability
  - Data and code availability
- EXPERIMENTAL MODEL AND SUBJECT DETAILS
  - Ethics statement
- METHOD DETAILS
  - Constructs and protein purification
  - Protein labeling with CoraFluor-1 or BODIPY FL
  - TR-FRET assay for RBD, S protein, N protein or total IgG
  - TR-FRET ACE2-Spike neutralization assay
  - ELISA assay for RBD protein, S protein or N protein
  - Cellular neutralization assay
- QUANTIFICATION AND STATISTICAL ANALYSIS

## SUPPLEMENTAL INFORMATION

Supplemental information can be found online at https://doi.org/10.1016/j.crmeth.2023.100421.

## ACKNOWLEDGMENTS

We would like to thank Dr. Xu Yu and the Massachusetts Coalition for Pandemic Readiness for additional samples provided by the Ragon Institute. We would like to thank Dr. Milka Kostic for critical reading of the manuscript. This work was supported by a philanthropic gift from Giving | Grousbeck Fazzalari (to E.S.F.), by NCI R01CA214608 (to E.S.F.), and by NSF 1830941 and NIH R21AI13298 (both to R.M.). E.S.F. is a Damon-Runyon Rachleff Investigator (DRR-50-18). Y.K. is supported by a grant from Japan Society for the Promotion of Science, a Grant-in-Aid for JSPS Fellows (20J01623), and Mochida Memorial Foundation for Medical and Pharmaceutical Research. N.C.P. is supported by the National Science Foundation Graduate Research Fellowship (DGE1745303). This work was supported by a gift from Ms. Enid

Schwartz and by the Mark and Lisa Schwartz Foundation, the Massachusetts Consortium for Pathogen Readiness, and the Ragon Institute of MGH, MIT, and Harvard. We thank all patients who provided samples.

## AUTHOR CONTRIBUTIONS

E.S.F., H.Y., R.P.N., and D.O. initiated the project, designed experiments, and analyzed data. H.Y., R.P.N., and D.O. performed ELISAs, developed and performed TR-FRET assays, and expressed and purified proteins and antibodies. N.C.P. and R.M. provided CoraFluor-1 reagents and helped with the optimization of protein labeling and assay conditions. S.F., C.A., and G.A. developed ELISAs and assisted with implementation at DFCI. Y.K., R.S.-P., L.K.B., L.R.B., E.J.N., E.W.K., X.G.Y, J.Z.L., and A.E.W. provided validated serum samples. E.C.L., K.S.D., and A.B.B. performed cellular neutralization assay and analyzed data. G.A., I.M.G., J.A.M., R.M., and E.S.F. supervised all aspects of the project and acquired funding. H.Y., R.P.N., and E.S.F. wrote the manuscript with input from all authors. All authors read, revised, and approved the manuscript.

## DECLARATION OF INTERESTS

E.S.F. is an equity holder and scientific advisor for Neomorph, Inc. (board member), Civetta Therapeutics, Proximity Therapeutics, Lighthorse Therapeutics, Avilar Therapeutics, and Photys Therapeutics and is a consultant to Novartis, Sanofi, AbbVie, Pfizer, Astellas, EcoR1 Capital, and Deerfield. The Fischer lab receives or has received research funding from Novartis, Ajax, Deerfield, and Astellas not related to this work. R.M. is a scientific advisory board (SAB) member and equity holder of Regenacy Pharmaceuticals, ERX Pharmaceuticals, and Frequency Therapeutics. H.Y., R.P.N., D.O., N.C.P., R.M., and E.S.F. are inventors on patent applications related to this work.

Received: September 2, 2022
Revised: December 15, 2022
Accepted: February 14, 2023
Published: February 20, 2023

## REFERENCES

1. Munster, V.J., Koopmans, M., van Doremalen, N., van Riel, D., and de Wit, E. (2020). A novel coronavirus emerging in China - key questions for impact assessment. N. Engl. J. Med. *382*, 692–694. https://doi.org/10.1056/NEJMp2000929.
2. Tang, Y.W., Schmitz, J.E., Persing, D.H., and Stratton, C.W. (2020). Laboratory diagnosis of COVID-19: current issues and challenges. J. Clin. Microbiol. *58*, e00512-20. https://doi.org/10.1128/JCM.00512-20.
3. Corradini, P., Gobbi, G., de Braud, F., Rosa, J., Rusconi, C., Apolone, G., and Carniti, C. (2020). Rapid antibody testing for SARS-CoV-2 in asymptomatic and paucisymptomatic healthcare professionals in hematology and oncology units identifies undiagnosed infections. Hemasphere *4*, e408. https://doi.org/10.1097/HS9.0000000000000408.
4. Ragó, Z., Szijjártó, L., Duda, E., and Bella, Z. (2020). [Opportunity of periodic monitoring of COVID-19 patients, asymptomatic virus carriers, and postinfectious individuals with IgM/IgG rapid antibody tests among healthcare workers during SARS-CoV-2 pandemic]. Orv. Hetil. *161*, 854–860. https://doi.org/10.1556/650.2020.31862.
5. Rodgers, M.A., Olivo, A., Harris, B.J., Lark, C., Luo, X., Berg, M.G., Meyer, T.V., Mohaimani, A., Orf, G.S., Goldstein, Y., et al. (2022). Detection of SARS-CoV-2 variants by Abbott molecular, antigen, and serological tests. J. Clin. Virol. *147*, 105080. https://doi.org/10.1016/j.jcv.2022.105080.
6. Konishi, Y., Sklavenitis-Pistofidis, R., Yue, H., Ferrari, F., Redd, R.A., Lightbody, E.D., Russo, M., Perry, J., Horowitz, E., Justis, A.V., et al. (2022). Attenuated response to SARS-CoV-2 vaccine in patients with asymptomatic precursor stages of multiple myeloma and Waldenstrom macroglobulinemia. Cancer Cell *40*, 6–8. https://doi.org/10.1016/j.ccell.2021.12.003.
7. Meyerhardt, J.A., Yue, H., Nowak, R.P., Brais, L., Ma, C., Johnson, S., Harrod, J., Burman, S.S.R., Hendrickson, L.M., Fischinger, S., et al. (2022). Serological testing for SARS-CoV-2 antibodies of employees shows low transmission working in a cancer center. PLoS One *17*, e0266791. https://doi.org/10.1371/journal.pone.0266791.
8. Amanat, F., Stadlbauer, D., Strohmeier, S., Nguyen, T.H.O., Chromikova, V., McMahon, M., Jiang, K., Asthagiri Arunkumar, G., Jurczyszak, D., Polanco, J., et al. (2020). A serological assay to detect SARS-CoV-2 seroconversion in humans. Preprint at medRxiv. https://doi.org/10.1101/2020.03.17.20037713.
9. Premkumar, L., Segovia-Chumbez, B., Jadi, R., Martinez, D.R., Raut, R., Markmann, A., Cornaby, C., Bartelt, L., Weiss, S., Park, Y., et al. (2020). The receptor binding domain of the viral spike protein is an immunodominant and highly specific target of antibodies in SARS-CoV-2 patients. Sci. Immunol. *5*, eabc8413. https://doi.org/10.1126/sciimmunol.abc8413.
10. Gruer, L., and Bhopal, R. (2020). Rapid roll out of SARS-CoV-2 antibody testing: even at high levels of specificity, an important proportion of test results will be false positives. BMJ *370*, m2910. https://doi.org/10.1136/bmj.m2910.
11. Malickova, K., Kratka, Z., Luxova, S., Bortlik, M., and Lukas, M. (2020). Anti-SARS-CoV-2 antibody testing in IBD healthcare professionals: are we currently able to provide COVID-free IBD clinics? Scand. J. Gastroenterol. *55*, 917–919. https://doi.org/10.1080/00365521.2020.1791244.
12. Özçürümez, M.K., Ambrosch, A., Frey, O., Haselmann, V., Holdenrieder, S., Kiehntopf, M., Neumaier, M., Walter, M., Wenzel, F., Wölfel, R., et al. (2020). SARS-CoV-2 antibody testing-questions to be asked. J. Allergy Clin. Immunol. *146*, 35–43. https://doi.org/10.1016/j.jaci.2020.05.020.
13. Theel, E.S., Slev, P., Wheeler, S., Couturier, M.R., Wong, S.J., and Kadkhoda, K. (2020). The role of antibody testing for SARS-CoV-2: is there one? J. Clin. Microbiol. *58*, 007977-20. https://doi.org/10.1128/JCM.00797-20.
14. Thornton, J.R., and Harel, A. (2020). Negative SARS-CoV-2 antibody testing following COVID-19 infection in Two MS patients treated with ocrelizumab. Mult. Scler. Relat. Disord. *44*, 102341. https://doi.org/10.1016/j.msard.2020.102341.
15. Infantino, M., Grossi, V., Lari, B., Bambi, R., Perri, A., Manneschi, M., Terenzi, G., Liotti, I., Ciotta, G., Taddei, C., et al. (2020). Diagnostic accuracy of an automated chemiluminescent immunoassay for anti-SARS-CoV-2 IgM and IgG antibodies: an Italian experience. J. Med. Virol. *92*, 1671–1675. https://doi.org/10.1002/jmv.25932.
16. Harritshøj, L.H., Gybel-Brask, M., Afzal, S., Kamstrup, P.R., Jørgensen, C.S., Thomsen, M.K., Hilsted, L., Friis-Hansen, L., Szecsi, P.B., Pedersen, L., et al. (2021). Comparison of 16 serological SARS-CoV-2 immunoassays in 16 clinical laboratories. J. Clin. Microbiol. *59*, 025966-20.
17. GeurtsvanKessel, C.H., Okba, N.M.A., Igloi, Z., Bogers, S., Embregts, C.W.E., Laksono, B.M., Leijten, L., Rokx, C., Rijnders, B., Rahamat-Langendoen, J., et al. (2020). An evaluation of COVID-19 serological assays informs future diagnostics and exposure assessment. Nat. Commun. *11*, 3436.
18. Egia-Mendikute, L., Bosch, A., Prieto-Fernández, E., Lee, S.Y., Jiménez-Lasheras, B., García Del Río, A., Antoñana-Vildosola, A., Bruzzone, C., Bizkarguenaga, M., Embade, N., et al. (2021). Sensitive detection of SARS-CoV-2 seroconversion by flow cytometry reveals the presence of nucleoprotein-reactive antibodies in unexposed individuals. Commun. Biol. *4*, 486.
19. Horndler, L., Delgado, P., Abia, D., Balabanov, I., Martínez-Fleta, P., Cornish, G., Llamas, M.A., Serrano-Villar, S., Sánchez-Madrid, F., Fresno, M., et al. (2021). Flow cytometry multiplexed method for the detection of neutralizing human antibodies to the native SARS-CoV-2 spike protein. EMBO Mol. Med. *13*, e13549.
20. Lapuente, D., Maier, C., Irrgang, P., Hübner, J., Peter, A.S., Hoffmann, M., Ensser, A., Ziegler, K., Winkler, T.H., Birkholz, T., et al. (2021). Rapid response flow cytometric assay for the detection of antibody responses to SARS-CoV-2. Eur. J. Clin. Microbiol. Infect. Dis. *40*, 751–759.

21. Dobaño, C., Vidal, M., Santano, R., Jiménez, A., Chi, J., Barrios, D., Ruiz-Olalla, G., Rodrigo Melero, N., Carolis, C., Parras, D., et al. (2021). Highly sensitive and specific multiplex antibody assays to quantify immunoglobulins M, A, and G against SARS-CoV-2 antigens. J. Clin. Microbiol. *59*, 017311-20.

22. Mariën, J., Ceulemans, A., Michiels, J., Heyndrickx, L., Kerkhof, K., Foque, N., Widdowson, M.-A., Mortgat, L., Duysburgh, E., Desombere, I., et al. (2021). Evaluating SARS-CoV-2 spike and nucleocapsid proteins as targets for antibody detection in severe and mild COVID-19 cases using a Luminex bead-based assay. J. Virol. Methods *288*, 114025.

23. Norman, M., Gilboa, T., Ogata, A.F., Maley, A.M., Cohen, L., Cai, Y., Zhang, J., Feldman, J.E., Hauser, B.M., Caradonna, T.M., et al. (2020). Ultra-sensitive high-resolution profiling of anti-SARS-CoV-2 antibodies for detecting early seroconversion in COVID-19 patients. Preprint at medRxiv. https://doi.org/10.1101/2020.04.28.20083691.

24. Woolley, C.F., and Hayes, M.A. (2013). Recent developments in emerging microimmunoassays. Bioanalysis *5*, 245–264. https://doi.org/10.4155/bio.12.298.

25. Lin, D., Liu, L., Zhang, M., Hu, Y., Yang, Q., Guo, J., Dai, Y., Xu, Y., Cai, Y., Chen, X., et al. (2020). Evaluations of the serological test in the diagnosis of 2019 novel coronavirus (SARS-CoV-2) infections during the COVID-19 outbreak. Eur. J. Clin. Microbiol. Infect. Dis. *39*, 2271–2277. https://doi.org/10.1007/s10096-020-03978-6.

26. Liu, A., Li, Y., Peng, J., Huang, Y., and Xu, D. (2021). Antibody responses against SARS-CoV-2 in COVID-19 patients. J. Med. Virol. *93*, 144–148. https://doi.org/10.1002/jmv.26241.

27. Lou, B., Li, T.D., Zheng, S.F., Su, Y.Y., Li, Z.Y., Liu, W., Yu, F., Ge, S.X., Zou, Q.D., Yuan, Q., et al. (2020). Serology characteristics of SARS-CoV-2 infection since exposure and post-symptom onset. Eur. Respir. J. *56*, 2000763. https://doi.org/10.1183/13993003.00763-2020.

28. Gorshkov, K., Vasquez, D.M., Chiem, K., Ye, C., Tran, B.N., de la Torre, J.C., Moran, T., Chen, C.Z., Martinez-Sobrido, L., and Zheng, W. (2021). A SARS-CoV-2 nucleocapsid protein TR-FRET assay amenable to high-throughput screening. Preprint at bioRxiv. https://doi.org/10.1101/2021.07.03.450938.

29. Ni, Y., Rosier, B.J.H.M., van Aalen, E.A., Hanckmann, E.T.L., Biewenga, L., Pistikou, A.M.M., Timmermans, B., Vu, C., Roos, S., Arts, R., et al. (2021). A plug-and-play platform of ratiometric bioluminescent sensors for homogeneous immunoassays. Nat. Commun. *12*, 4586. https://doi.org/10.1038/s41467-021-24874-3.

30. Yao, Z., Drecun, L., Aboualizadeh, F., Kim, S.J., Li, Z., Wood, H., Valcourt, E.J., Manguiat, K., Plenderleith, S., Yip, L., et al. (2021). A homogeneous split-luciferase assay for rapid and sensitive detection of anti-SARS CoV-2 antibodies. Nat. Commun. *12*, 1806. https://doi.org/10.1038/s41467-021-22102-6.

31. McGiven, J.A., Thompson, I.J., Commander, N.J., and Stack, J.A. (2009). Time-resolved fluorescent resonance energy transfer assay for simple and rapid detection of anti-Brucella antibodies in ruminant serum samples. J. Clin. Microbiol. *47*, 3098–3107. https://doi.org/10.1128/JCM.00919-09.

32. Rusanen, J., Kareinen, L., Szirovicza, L., Uğurlu, H., Levanov, L., Jääskeläinen, A., Ahava, M., Kurkela, S., Saksela, K., Hedman, K., et al. (2021). A generic, scalable, and rapid time-resolved forster resonance energy transfer-based assay for antigen detection-SARS-CoV-2 as a proof of concept. mBio *12*, e00902-21. https://doi.org/10.1128/mBio.00902-21.

33. Cecon, E., Burridge, M., Cao, L., Carter, L., Ravichandran, R., Dam, J., and Jockers, R. (2022). SARS-COV-2 spike binding to ACE2 in living cells monitored by TR-FRET. Cell Chem. Biol. *29*, 74–83.e4. https://doi.org/10.1016/j.chembiol.2021.06.008.

34. Payne, N.C., Kalyakina, A.S., Singh, K., Tye, M.A., and Mazitschek, R. (2021). Bright and stable luminescent probes for target engagement profiling in live cells. Nat. Chem. Biol. *17*, 1168–1177. https://doi.org/10.1038/s41589-021-00877-5.

35. Li, W., Moore, M.J., Vasilieva, N., Sui, J., Wong, S.K., Berne, M.A., Somasundaran, M., Sullivan, J.L., Luzuriaga, K., Greenough, T.C., et al. (2003). Angiotensin-converting enzyme 2 is a functional receptor for the SARS coronavirus. Nature *426*, 450–454.

36. Chen, X., Li, R., Pan, Z., Qian, C., Yang, Y., You, R., Zhao, J., Liu, P., Gao, L., Li, Z., et al. (2020). Human monoclonal antibodies block the binding of SARS-CoV-2 spike protein to angiotensin converting enzyme 2 receptor. Cell. Mol. Immunol. *17*, 647–649.

37. ter Meulen, J., van den Brink, E.N., Poon, L.L.M., Marissen, W.E., Leung, C.S.W., Cox, F., Cheung, C.Y., Bakker, A.Q., Bogaards, J.A., van Deventer, E., et al. (2006). Human monoclonal antibody combination against SARS coronavirus: synergy and coverage of escape mutants. PLoS Med. *3*, e237. https://doi.org/10.1371/journal.pmed.0030237.

38. Tian, X., Li, C., Huang, A., Xia, S., Lu, S., Shi, Z., Lu, L., Jiang, S., Yang, Z., Wu, Y., and Ying, T. (2020). Potent binding of 2019 novel coronavirus spike protein by a SARS coronavirus-specific human monoclonal antibody. Emerg. Microbes Infect. *9*, 382–385. https://doi.org/10.1080/22221751.2020.1729069.

39. Ha, S.H., Kim, S.Y., and Ferrell, J.E., Jr. (2016). The prozone effect accounts for the paradoxical function of the Cdk-binding protein Suc1/Cks. Cell Rep. *16*, 2047. https://doi.org/10.1016/j.celrep.2016.07.073.

40. Douglass, E.F., Jr., Miller, C.J., Sparer, G., Shapiro, H., and Spiegel, D.A. (2013). A comprehensive mathematical model for three-body binding equilibria. J. Am. Chem. Soc. *135*, 6092–6099. https://doi.org/10.1021/ja311795d.

41. McDade, T.W., McNally, E., Zelikovich, A., D'Aquila, R., Mustanski, B., Miller, A., Vaught, L., Reiser, N., Bogdanovic, E., and Fallon, K. (2020). High seroprevalence for SARS-CoV-2 among household members of essential workers detected using a dried blood spot assay. Preprint at medRxiv. https://doi.org/10.1101/2020.06.01.20119602.

42. Roy, V., Fischinger, S., Atyeo, C., Slein, M., Loos, C., Balazs, A., Luedemann, C., Astudillo, M.G., Yang, D., Wesemann, D.R., et al. (2020). SARS-CoV-2-specific ELISA development. J. Immunol. Methods *484–485*, 112832. https://doi.org/10.1016/j.jim.2020.112832.

43. Nilles, E.J., Karlson, E.W., Norman, M., Gilboa, T., Fischinger, S., Atyeo, C., Zhou, G., Bennett, C.L., Tolan, N.V., and Oganezova, K. (2020). Evaluation of two commercial and two non-commercial immunoassays for the detection of prior infection to SARS-CoV-2. Preprint at medRxiv. https://doi.org/10.1101/2020.06.24.20139006.

44. FDA (2021). Policy for coronavirus disease-2019 tests during the public health emergency (revised). https://www.fda.gov/regulatory-information/search-fda-guidance-documents/policy-coronavirus-disease-2019-tests-during-public-health-emergency-revised.

45. Dutta, N.K., Mazumdar, K., and Gordy, J.T. (2020). The nucleocapsid protein of SARS-CoV-2: a target for vaccine development. J. Virol. *94*, 006477-20. https://doi.org/10.1128/JVI.00647-20.

46. Lu, R., Zhao, X., Li, J., Niu, P., Yang, B., Wu, H., Wang, W., Song, H., Huang, B., Zhu, N., et al. (2020). Genomic characterisation and epidemiology of 2019 novel coronavirus: implications for virus origins and receptor binding. Lancet *395*, 565–574. https://doi.org/10.1016/S0140-6736(20)30251-8.

47. Narayanan, K., Chen, C.J., Maeda, J., and Makino, S. (2003). Nucleocapsid-independent specific viral RNA packaging via viral envelope protein and viral RNA signal. J. Virol. *77*, 2922–2927. https://doi.org/10.1128/jvi.77.5.2922-2927.2003.

48. Seow, J., Graham, C., Merrick, B., Acors, S., Pickering, S., Steel, K.J.A., Hemmings, O., O'Byrne, A., Kouphou, N., Galao, R.P., et al. (2020). Longitudinal observation and decline of neutralizing antibody responses in the three months following SARS-CoV-2 infection in humans. Nat. Microbiol. *5*, 1598–1607.

49. Zohar, T., Loos, C., Fischinger, S., Atyeo, C., Wang, C., Slein, M.D., Burke, J., Yu, J., Feldman, J., Hauser, B.M., et al. (2020). Compromised humoral functional evolution tracks with SARS-CoV-2 mortality. Cell *183*, 1508–1519.e12. https://doi.org/10.1016/j.cell.2020.10.052.

50. Li, F. (2016). Structure, function, and evolution of coronavirus spike proteins. Annu. Rev. Virol. *3*, 237–261.

51. Cueno, M.E., and Imai, K. (2020). Structural comparison of the SARS CoV 2 spike protein relative to other human-infecting coronaviruses. Front. Med. *7*, 594439.

52. Hatmal, M.M., Alshaer, W., Al-Hatamleh, M.A.I., Hatmal, M., Smadi, O., Taha, M.O., Oweida, A.J., Boer, J.C., Mohamud, R., and Plebanski, M. (2020). Comprehensive structural and molecular comparison of spike proteins of SARS-CoV-2, SARS-CoV and MERS-CoV, and their interactions with ACE2. Cells *9*, 2638.

53. Zhu, Y., Yu, D., Han, Y., Yan, H., Chong, H., Ren, L., Wang, J., Li, T., and He, Y. (2020). Cross-reactive neutralization of SARS-CoV-2 by serum antibodies from recovered SARS patients and immunized animals. Sci. Adv. *6*, eabc9999.

54. Gonzalez-Quintela, A., Alende, R., Gude, F., Campos, J., Rey, J., Meijide, L.M., Fernandez-Merino, C., and Vidal, C. (2008). Serum levels of immunoglobulins (IgG, IgA, IgM) in a general adult population and their relationship with alcohol consumption, smoking and common metabolic abnormalities. Clin. Exp. Immunol. *151*, 42–50. https://doi.org/10.1111/j.1365-2249.2007.03545.x.

55. Hoffmann, M., Kleine-Weber, H., Schroeder, S., Krüger, N., Herrler, T., Erichsen, S., Schiergens, T.S., Herrler, G., Wu, N.H., Nitsche, A., et al. (2020). SARS-CoV-2 cell entry depends on ACE2 and TMPRSS2 and is blocked by a clinically proven protease inhibitor. Cell *181*, 271–280.e8. https://doi.org/10.1016/j.cell.2020.02.052.

56. Nie, J., Li, Q., Wu, J., Zhao, C., Hao, H., Liu, H., Zhang, L., Nie, L., Qin, H., Wang, M., et al. (2020). Establishment and validation of a pseudovirus neutralization assay for SARS-CoV-2. Emerg. Microbes Infect. *9*, 680–686. https://doi.org/10.1080/22221751.2020.1743767.

57. Wu, Y., Wang, F., Shen, C., Peng, W., Li, D., Zhao, C., Li, Z., Li, S., Bi, Y., Yang, Y., et al. (2020). A noncompeting pair of human neutralizing antibodies block COVID-19 virus binding to its receptor ACE2. Science *368*, 1274–1278. https://doi.org/10.1126/science.abc2241.

58. Garcia-Beltran, W.F., Lam, E.C., Astudillo, M.G., Yang, D., Miller, T.E., Feldman, J., Hauser, B.M., Caradonna, T.M., Clayton, K.L., Nitido, A.D., et al. (2021). COVID-19-neutralizing antibodies predict disease severity and survival. Cell *184*, 476–488.e11.

59. Tan, C.W., Chia, W.N., Qin, X., Liu, P., Chen, M.I.C., Tiu, C., Hu, Z., Chen, V.C.W., Young, B.E., Sia, W.R., et al. (2020). A SARS-CoV-2 surrogate virus neutralization test based on antibody-mediated blockage of ACE2-spike protein-protein interaction. Nat. Biotechnol. *38*, 1073–1078. https://doi.org/10.1038/s41587-020-0631-z.

60. Abe, K.T., Li, Z., Samson, R., Samavarchi-Tehrani, P., Valcourt, E.J., Wood, H., Budylowski, P., Dupuis, A.P., 2nd, Girardin, R.C., Rathod, B., et al. (2020). A simple protein-based surrogate neutralization assay for SARS-CoV-2. JCI Insight *5*, e142362. https://doi.org/10.1172/jci.insight.142362.

61. Engvall, E., and Perlmann, P. (1971). Enzyme-linked immunosorbent assay (ELISA). Quantitative assay of immunoglobulin G. Immunochemistry *8*, 871–874. https://doi.org/10.1016/0019-2791(71)90454-x.

62. Cohen, L., and Walt, D.R. (2017). Single-molecule arrays for protein and nucleic acid analysis. Annu. Rev. Anal. Chem. *10*, 345–363. https://doi.org/10.1146/annurev-anchem-061516-045340.

## STAR★METHODS

### KEY RESOURCES TABLE

| REAGENT or RESOURCE | SOURCE | IDENTIFIER |
|---|---|---|
| Antibodies | | |
| αhs-IgG | Bethyl Laboratory | Cat# A80-104A; RRID: AB_67061 |
| αhs-IgM | Bethyl Laboratory | Cat# A80-100A; RRID: AB_67079 |
| αhs-IgA | Bethyl Laboratory | Cat# A80-102A; RRID: AB_67044 |
| B38 | Laboratory of Eric S. Fischer | This study |
| H4 | Laboratory of Eric S. Fischer | This study |
| HRP-anti human IgG | Bethyl Laboratory | Cat# A80-104P; RRID: AB_67064 |
| HRP-anti human IgA | Bethyl Laboratory | Cat# A80-100P; RRID: AB_67082 |
| HRP-anti human IgM | Bethyl Laboratory | Cat# A80-102P; RRID: AB_67047 |
| CR3022 IgG | Laboratory of Eric S. Fischer | This study |
| CR3022 IgM | Laboratory of Eric S. Fischer | This study |
| CR3022 IgA | Laboratory of Eric S. Fischer | This study |
| Protein G | GE | GE17-0405-01 |
| AF488-Nanobody (CTK0101, Nano-Secondary, ChromoTek) | Laboratory of Ralph Mazitschek | This study |
| Biological samples | | |
| Serological sample | hospitalized patients (MGH and BWH) with a SARS-CoV-2 confirmed RNA tests | This study |
| Serological sample | convalescents patients (MGH) with a confirmed prior SARS-CoV-2 RNA+ and two repeat RNA-negative tests after 2 weeks of isolation | This study |
| Serological sample | pre-pandemic healthy controls with samples collected prior to December 1, 2019 (MGB Biobank); | This study |
| Serological sample | a group of low-risk community members (Ragon Institute) | This study |
| Serological sample | Self-collection samples from DFCI employees (DFCI IRB #20-260) | This study |
| Serological sample | The IMPACT study (DFCI IRB #20-332) patients samples with or without vaccination | This study |
| Chemicals, peptides, and recombinant proteins | | |
| Full-length Spike protein of SARS-CoV-2 | LakePharma | Cat# 46328 |
| RBD of SARS-CoV-2 | LakePharma | Cat# 46438 |
| Full-length biotinylated N protein of SARS-CoV-2 (construct 1-419 with N terminal His-Avi tag) | Acro Biosystem | Cat# NUN-C81Q6 |
| Full-length Spike protein of SARS-CoV | Sino Biological | Cat# 40634-V08B |
| Full-length Spike protein of MERS-CoV | Sino Biological | Cat# 40069-V08B |
| Biotinylated N-protein of SARS-CoV-2 | Laboratory of Eric S. Fischer | This study |
| Biotinylated ACE2 (18-615) | Laboratory of Eric S. Fischer | This study |
| CoraFluor-1-Pfp | Laboratory of Ralph Mazitschek | Payne et al.[34] |
| BODIPY FL-NHS | Thermo Fisher Scientific | Cat# D2184 |
| Experimental models: Cell lines | | |
| Expi293 expression systerm | Thermo Fisher Scientific | Cat# A14635 |
| Hi5 | Thermo Fisher Scientific | Cat# B85502 |

(*Continued on next page*)

*Continued*

| REAGENT or RESOURCE | SOURCE | IDENTIFIER |
|---|---|---|
| Recombinant DNA | | |
| H3 | Laboratory of Eric S. Fischer | This study |
| B38 | Laboratory of Eric S. Fischer | This study |
| CR3022 IgG | Laboratory of Eric S. Fischer | This study |
| CR3022 IgM | Laboratory of Eric S. Fischer | This study |
| CR3022 IgA | Laboratory of Eric S. Fischer | This study |
| N protein | Laboratory of Eric S. Fischer | This study |
| ACE2 | Laboratory of Eric S. Fischer | This study |
| Software and algorithms | | |
| GraphPad Prism | Graphpad Software Inc | https://www.graphpad.com/scientific-software/prism/ |
| Adobe Illustrator | Adobe | https://www.adobe.com/products/illustrator |

## RESOURCE AVAILABILITY

### Lead contact

Further information and requests for resources and reagents should be directed to and will be fulfilled by the lead contact, Dr. Eric S. Fischer (eric_fischer@dfci.harvard.edu).

### Materials availability

CoraFluor-1-Pfp has been licensed to Tocris Bioscience and will be commercially available in the near future. As an academic institution, MGH will also grant non-exclusive research licenses to other academic institutions. Plasmids, purified proteins, and reagents newly generated for this study are indicated in the key resources table and are available from the lead contact upon request.

### Data and code availability

- All data reported in this paper will be shared by the lead contact upon request.
- This paper does not report original code.
- Any additional information required to reanalyze the data reported in this paper is available from the lead contact upon request.

## EXPERIMENTAL MODEL AND SUBJECT DETAILS

### Ethics statement

Serum/plasma samples used in this study were obtained through the Massachusetts Consortium on Pathogen Readiness (MassCPR) from Mass General Hospital (MGH), Brigham and Women's Hospital (BWH) through the Mass General Brigham (MGB) Biobank, through the Ragon Institute and Dana-Farber Cancer Institute (DFCI). The summary of the cohorts is presented in Table S1. Institutional IRB approval was obtained, and all samples were collected after subjects provided signed informed consent. Six groups of consented subjects were included: 1) hospitalized patients (MGH and BWH) with a SARS-CoV-2 confirmed RNA tests[42]; 2) convalescents patients (MGH) with a confirmed prior SARS-CoV-2 RNA+ and two repeat RNA-negative tests after 2 weeks of isolation[42]; 3) pre-pandemic healthy controls with samples collected prior to December 1, 2019 (MGB Biobank, Crimson Study ID: T0764); 4) a group of low-risk community members (Ragon); 5) Self-collection samples from DFCI employees (DFCI IRB #20-260); 6) The IMPACT study (DFCI IRB #20-332) patients samples with or without vaccination. Total IgG levels of IMPACT study samples were available from medical records. Samples were heat inactivated at 60°C for 1 hour.

## METHOD DETAILS

### Constructs and protein purification

Antibodies were expressed in Expi293T cells following manufacturer protocol (Thermo Fisher Scientific, A14525) with transfection ratios of 1:1 or 2:1 of heavy to light chain. The cell suspension was cleared using centrifugation, 15 min at 40k rpm Ti45, Beckman Coulter). The clarified media was filtered with 0.45 μm filter before binding to either protein G (GE, GE17-0405-01) for IgG, protein L (GE, GE17-5478-15) for IgM or peptide M (InvivoGen, gel-pdm-5) for IgA1 columns pre-equilibrated with binding buffer (PBS, 10 mM $Na_2HPO_4$, 1.8 mM $KH_2PO_4$, 137 mM NaCl, 2.7 mM KCl at pH 7.4). The beads were washed with 20-50 column volumes of binding buffer. The protein was eluted from the beads with 6-15 column volumes of 0.1 M glycine pH 3.0 elution buffer and immediately

quenched using a 10:1 ratio of 1 M Tris-HCl pH 8.0. The protein-containing fractions were pooled and flash-frozen in liquid nitrogen at 0.1–1.5 mg/mL. The antibodies were stored at −80°C until further use. Concentrations were estimated using Bradford assay. CR3022 IgG was labeled with BODIPY FL-NHS as described below.

Neutralizing antibodies B38 and H4 Fab fragments were constructed using the CR3022 Fc regions. The Fab fragment sequence was taken from Wu, Y. et al.[57] B38 and H4 antibodies were expressed in Expi293T and purified as described above for CR3022.

A truncated ACE2 (amino acids 18–615) without a signaling peptide was cloned and expressed in Hi-5 insect cells by using baculoviruses with C-terminal StrepII and avi fusion tags. The full-length expressed in insect cells with an N-terminal StrepII-Avi-TEV fusion tag. For both purifications cells were lysed by sonication (in 50 mM Tris pH 8.0, 200 mM NaCl, 0.1% Triton X-100, 1 mM PMSF and 1 tablet of complete protease inhibitor cocktail Roche Applied Science), lysate cleared by high-speed centrifugation, and the supernatant passed over StrepTactin-XT HC affinity resin (IBA). Target protein was eluted using biotin and subjected to Poros50HQ ion-exchange chromatography. Purification was completed using size exclusion chromatography with a HiLoad 16/600 Superdex 200 (GE Healthcare) in 50 mM HEPES pH 7.4, 200 mM NaCl and 2 mM TCEP. The purified avi-tagged ACE2 protein or avi-tagged N protein was biotinylated in presence of BirA enzyme, 10 mM $MgCl_2$, 2 mM biotin, 20 mM ATP. Biotinylation was confirmed by mass spectrometry. The protein-containing fractions were pooled and flash-frozen in liquid nitrogen at 0.9 mg/mL for ACE2 and 1.6 mg/mL for N protein. The proteins were stored at −80°C until further use. Concentrations were estimated using Bradford assay.

### Protein labeling with CoraFluor-1 or BODIPY FL

2.5 mL αhs-IgG (Bethyl, A80-104A), αhs-IgM (Bethyl, A80-100A), αhs-IgA (Bethyl, A80-102A), S protein (LakePharma, 46328), protein G (Life, 21193) or RBD protein (LakePharma, 46438) at a concentration of 1 mg/mL or SARS-CoV S protein (Cat. 40634-V08B) and MERS-CoV S protein (Cat. 40069-V08B) at concentration of 0.25 mg/mL was buffer exchanged into 100 mM sodium carbonate buffer at pH 8.5, 0.05% TWEEN 20 using PD-10 Desalting Columns (Sigma, GE17-0851-01) according to the manufacturer's protocol with 0.5 mL per elution fraction. Protein-containing fractions were pooled at 0.5–1 mg/mL and the appropriate volume of either CoraFluor-1-Pfp[34] (1 mM in dimethylacetamide (DMAc)) or BODIPY FL-NHS (at 10 mM concentration in DMSO) was added to achieve a molar ratio of approximately 4-5x CoraFluor-1-Pfp or 6x BODIPY FL. The reaction mixture was briefly vortexed and allowed to stand at room temperature for 1 h. To purify the labeled conjugates, the labeling reaction was buffer exchanged into 50 mM sodium phosphate buffer pH 7.4, 137 mM NaCl, 0.05% TWEEN 20 using PD-10 desalting columns following manufacturer protocol using 0.5 mL elution fractions. Protein-containing fractions were pooled and flash-frozen in liquid nitrogen at 0.4–0.6 mg/mL concentration and stored at −80°C.

The corrected $A_{280}$ value ($A_{280,corr}$) of protein conjugate was determined via Nanodrop (0.1 cm path length) by measuring $A_{280}$ and $A_{340}$, using Equation 1:

$$A_{280,corr} = A_{280} - (A_{340} \times cf) \quad \text{(Equation 1)}$$

where *cf* is the correction factor for the CoraFluor-1 contribution to $A_{280}$ and is equal to 0.157.

The concentration of protein conjugate, $c_p$ (M) was determined using Equation 2:

$$c_p = \frac{A_{280,corr}}{\varepsilon b} \quad \text{(Equation 2)}$$

where ε is the antibody extinction coefficient at $A_{280}$, equal to 210,000 $M^{-1}cm^{-1}$ for IgG class anti IgG/IgM/IgA Ab, 240,000 $M^{-1}cm^{-1}$ for S protein, 80,200 $M^{-1}cm^{-1}$ for RBD and *b* is path length in cm (0.1 cm).

The concentration of Tb complex, $c_{Tb}$ (M) covalently bound to the proteins was determined using Equation 3:

$$c_{Tb} = \frac{A_{340}}{\varepsilon b} \quad \text{(Equation 3)}$$

where ε is the complex extinction coefficient at $A_{340}$, equal to 22,000 $M^{-1}cm^{-1}$ and *b* is path length in cm (0.1 cm).

The degree of labeling (*DOL*) was calculated using Equation 4:

$$DOL = \frac{c_{Tb}}{c_p} \quad \text{(Equation 4)}$$

### TR-FRET assay for RBD, S protein, N protein or total IgG

Titration of CR3022 IgG/IgM/IgA1 antibody or dilution of tested human serum samples was added to assay mix with final concentrations of 15 nM CoraFluor-1-labeled RBD and 250 nM BODIPY FL-labeled αIgG/αIgM/αIgA, or 7.5 nM CoraFluor-1-labeled S protein of SARS-CoV-2, SARS-CoV or MERS-CoV, 250 nM BODIPY FL-labeled αIgG/αIgM/αIgA, or 2 nM Streptavidin-CoraFluor-1 and 250 nM BODIPY FL-labeled αIgG, or 25 nM CoraFluor-1-Protein G and 25 nM AF488 labeled Nanobodies in a buffer containing PBS, 0.05% TWEEN 20 (Sigma Aldrich P9416). Serum/plasma/whole blood samples were diluted in the buffer containing 50 mM Tris-HCl pH 8.0, 140 mM NaCl, 0.05% TWEEN 20 and 1% BSA (Cell Signaling Technology 9998S) to the final assay condition of 1:150 (v/v). The assay was prepared by combining 5 μL of 3x assay mix with 10 μL of 1:100 (v/v) of sample. TR-FRET assays were performed in

384-well microplate (Corning, 4514) with 15 μL final assay volume. Before TR-FRET measurements were conducted, the reactions were incubated for 1h at RT. After excitation of CoraFluor-1 (Tb) fluorescence at 337 nm, emission at 490 nm (CoraFluor-1) and 520 nm (BODIPY FL) were recorded with a 70 μs delay over 130 μs to reduce background fluorescence and the reaction was followed over >20 or >100 s cycles of each data point using a PHERAstar FS microplate reader (BMG Labtech). The TR-FRET signal of each data point was extracted by calculating the 520/490 nm ratio.

### TR-FRET ACE2-Spike neutralization assay

Dilution of human serum samples were added to assay mix with final concentrations of 8 nM Biotinylated ACE2 protein, 2 nM Streptavidin-CoraFluor-1 and 8 nM BODIPY FL-labeled Spike in a buffer containing PBS, 0.05% TWEEN 20 (Sigma Aldrich P9416). Serum samples were diluted in the buffer containing 50 mM Tris pH 8.0, 140 mM NaCl, 0.05% TWEEN 20 and 1% BSA (Cell Signaling Technology 9998S) to the final assay concentration of 1:50 (v/v) or as a full dose response titration. TR-FRET assays were performed in 384-well microplates (Corning, 4514) with 15 μL final assay volume. Biotinylated ACE2 protein and Streptavidin-CoraFluor-1 (mix 1) were premixed and incubated for 10 min at RT. BODIPY FL-Spike protein and antibody or serum samples (mix 2) were pre-incubated for 30 min at RT. Mix 1 and 2 were added together and before TR-FRET measurements were conducted, the reactions were incubated for 1 to 4 h at RT. After excitation of CoraFluor-1 (Tb) fluorescence at 337 nm, emission at 490 nm (CoraFluor-1) and 520 nm (BODIPY FL) were recorded with a 70 μs delay over 130 μs to reduce background fluorescence. The reaction was followed over >20 or >100 s cycles of each data point using a PHERAstar FS microplate reader (BMG Labtech). The TR-FRET signal of each data point was extracted by calculating the 520/490 nm ratio. The AUC was calculated as the sum of the averages of duplicate individual 8-point dose-response data points.

### ELISA assay for RBD protein, S protein or N protein

384-well ELISA plates (ThermoFisher #464718) were coated with 50 μL/well of 500 ng/mL SARS-CoV-2-RBD or SARS-CoV-2 S protein or SARS-CoV-2 N protein in coating buffer (1 capsule of carbonate-bicarbonate buffer (Sigma #C3041100CAP) per 100 mL Milli-Q H2O) for 30 min at room temperature. Plates were then washed 3 times with 100 μL/well of wash buffer (0.05% TWEEN 20, 400 mM NaCl, 50 mM Tris pH 8.0 in Milli-Q H2O) using a Tecan automated plate washer. Plates were blocked by adding 100 μL/well of blocking buffer (1% BSA, 140 mM NaCl, 50 mM Tris pH 8.0 in Milli-Q H2O) for 30 min at room temperature. Plates were then washed as described above. 50 μL of diluted serum samples (in dilution buffer; 1% BSA, 0.05% TWEEN 20, 140 mM NaCl, 50 mM Tris (pH 8.0) in Milli-Q H2O) was added to the wells and incubated for 30 min at 37°C. Plates were then washed 5 times as described above. 50 μL/well of diluted detection antibody solution (HRP-anti human IgG Bethyl Laboratory #A80-104P) was added to the wells and incubated for 30 min at room temperature. Plates were then washed 5 times as described above. 40 μL/well of TMB peroxidase substrate (Thermo Fisher #34029) was then added to the wells and incubated at room temperature for 3 min (αIgG). The reaction was stopped by adding 40 μL/well of stop solution (1 M H2SO4 in Milli-Q H2O) to each well. OD was read at 450 nm and 570 nm on a PHERAstar FSX plate reader (BMG Labtech). The final data used in the analysis was calculated by subtracting 570 nm background from 450 nm signal.

### Cellular neutralization assay

Lentiviral particles pseudotyped with SARS-CoV-2 spike protein were produced by transient transfection of 293T cells and titered by flow cytometry on 293T-ACE2 cells. Neutralization assays were performed on a Fluent Automated Workstation (Tecan) using 384-well plates (Greiner, 781,090). Following an initial 12-fold dilution, the liquid handler performed serial 3-fold dilutions (ranging from 1:12 to 1:8,748) of each patient serum and/or purified antibody in 20 μl followed by addition of 20 μL of pseudovirus containing 125 infectious units and incubation for 1 h at room temperature. Finally, 10,000 293T-ACE2 cells in 20 μL cell media containing 15 μg/mL polybrene were added to each well and incubated at 37°C for 60–72 h. Following transduction, cells were lysed using a modified form of a previously described assay buffer containing a final concentration of 20 mM Tris-HCl, 100 μM EDTA, 1.07 mM $MgCl_2$, 2.67–26.7 mM $MgSO_4$, 17 mM dithiothreitol (DTT), 250 μM ATP, and 125–250 μM D-luciferin, 1% Triton X- and shaken for 5 min prior to quantitation of luciferase expression within 1h of buffer addition using a Spectramax L luminometer (Molecular Devices). Percent neutralization was determined by subtracting background luminescence measured in cell control wells (cells only) from sample wells and dividing by virus control wells (virus and cells only). Data was analyzed using Graphpad Prism and NT50 values were calculated by taking the inverse of the 50% inhibitory concentration value for all samples with a neutralization value of 80% or higher at the highest concentration of serum or antibody.

## QUANTIFICATION AND STATISTICAL ANALYSIS

Statistical calculations were performed using Prism 8.0.2 and R v3.6.1; packages ggplot2. The samples in ELISA IgG or TR-FRET IgG were classified as positive if the value exceeded the mean (Healthy) + 3 SD (Healthy) threshold.